



**Synthesis and evaluation of 6-substituted 3-arylcoumarin derivatives as multifunctional acetylcholinesterase/monoamine oxidase B dual inhibitors for the treatment of Alzheimer's disease**

Journal:	<i>RSC Advances</i>
Manuscript ID	RA-ART-10-2015-022296.R1
Article Type:	Paper
Date Submitted by the Author:	17-Nov-2015
Complete List of Authors:	Wang, Zhi-Min; China Pharmaceutical University, Natural Medicinal Chemistry Li, Xue-mei; China Pharmaceutical University, Department of Natural Medicinal Chemistry Xue, Gui-Min; China Pharmaceutical University Xu, Wei; China Pharmaceutical University, Department of Natural Medicinal Chemistry Wang, Xiao-Bing; China Pharmaceutical University, Department of Natural Medicinal Chemistry; China Pharmaceutical university, Kong, Ling-Yi; China Pharmaceutical University, Department of Natural Medicinal Chemistry
Subject area & keyword:	Bioorganic chemistry < Chemical biology & medicinal

**Synthesis and evaluation of 6-substituted 3-arylcoumarin derivatives  
as multifunctional acetylcholinesterase/monoamine oxidase B dual  
inhibitors for the treatment of Alzheimer's disease**

Zhi-Min Wang, Xue-Mei Li, Gui-Min Xue, Wei Xu, Xiao-Bing Wang\* and Ling-Yi Kong\*

*State Key Laboratory of Natural Medicines, Department of Natural Medicinal Chemistry, China Pharmaceutical University, 24 Tong Jia Xiang, Nanjing 210009, People's Republic of China*

\* *Corresponding Authors. Tel/Fax: +86-25-83271405; E-mail: cpu\_lykong@126.com (Ling-Yi Kong); xbwang@cpu.edu.cn.*

**Abstract**

Considering the complex etiology of Alzheimer's disease (AD), multifunctional agents may represent important properties against this disease. A series of 6-substituted 3-arylcoumarins (**5a-t**) were designed, synthesized and evaluated as cholinesterase (ChE) and monoamino oxidase (MAO) inhibitors. Among them, compounds **5o** [IC<sub>50</sub>, 195 nM for hAChE, SI (hBuChE/hAChE) = 145; IC<sub>50</sub>, 63.5 nM for hMAO-B, SI (hMAO-A/hMAO-B) = 25] and **5p** [IC<sub>50</sub>, 185 nM for hAChE, SI (hBuChE/hAChE) = 182; IC<sub>50</sub>, 196 nM for hMAO-B, SI (hMAO-A/hMAO-B) > 510] selectively inhibited both hAChE and hMAO-B with IC<sub>50</sub> values in the nanomolar range. The abilities of **5o** and **5p** binding to hAChE and hMAO-B were confirmed by molecular docking and kinetic studies. Moreover, **5o** and **5p** exhibited significant inhibition of self-induced A $\beta$ <sub>42</sub> aggregation (61% and 52%, at 20  $\mu$ M), antioxidant (0.81 and 1.17 trolox equivalent by ABTS assay), neuroprotection against A $\beta$ <sub>42</sub>-induced cytotoxicity and BBB penetration capacity (PAMPA-BBB+), were potential anti-Alzheimer agents with balanced activities. Overall, the study provided meaningful information for further development of multifunctional drugs for AD therapy.

**Keywords:** Alzheimer's disease, 3-arylcoumarin derivatives, Cholinesterase inhibitors, Monoamine oxidase,  $\beta$ -Amyloid aggregation.

## 1. Introduction

Alzheimer's disease (AD), an age-related neurodegenerative disease, is characterized by memory loss, decline in language skills and other cognitive impairments<sup>1</sup>. Although the pathology of AD is not completely known,  $\beta$ -amyloid ( $A\beta$ ) protein deposits<sup>2</sup>, cholinergic neurons system dysfunction<sup>3</sup>, oxidative stress<sup>4</sup>,  $\tau$ -protein hyperphosphorylation and metal dyshomeostasis<sup>5, 6</sup> are thought to play significant roles in the pathophysiology of the disease.

The cholinergic hypothesis suggests that the cognitive and memory deteriorations associated with AD are caused by the selective decline of acetylcholine (ACh)<sup>7</sup>. The primary approach of AD therapy has therefore focused on increasing the brain ACh levels by treating with acetylcholinesterase inhibitors (AChEI). AChEIs such as tacrine<sup>8</sup>, rivastigmine<sup>9</sup>, galantamine<sup>10</sup>, and donepezil have shown a modest improvement in cognitive and memory function<sup>11</sup>. The X-ray crystallographic structure of AChE reveals that it contains two binding sites: the catalytic active site (CAS) and the peripheral anionic site (PAS) connected by a deep hydrophobic gorge<sup>12</sup>. Generally, inhibitors that bind to either one of these sites can inhibit AChE. Current studies indicate that the PAS of AChE not only facilitates cholinergic transmission but also accelerates deposition and aggregation of  $A\beta$ <sup>13</sup>. The aggregation of  $A\beta$  leads to the formation of senile plaques, resulting in neuronal dysfunction in AD patients<sup>14, 15</sup>. Two main  $A\beta$  isoforms ( $A\beta_{40}$  and  $A\beta_{42}$ ) are primarily generated by the sequential cleaving of the amyloid precursor protein (APP) by  $\beta$ - and  $\gamma$ -secretases.  $A\beta_{42}$  is the predominant form in senile plaques, having lower solubility

and stronger neuronal toxicity than  $A\beta_{40}$ . Therefore, the inhibition of  $A\beta_{42}$  aggregation is another potential approach for the treatment of AD<sup>16-18</sup>.

In addition, it has been reported that monoamine oxidase (MAO; EC 1.4.3.4), is also an important target for the treatment of AD<sup>19</sup>. MAO, existed as two isozymes, MAO-A and MAO-B, is a flavoenzyme that catalyzes the deamination of amines and is responsible for the regulation and metabolism of major monoamine neurotransmitters<sup>20-22</sup>. MAO-A is involved in psychiatric conditions and depression, whereas MAO-B accelerates the oxidative deamination of neurotransmitters, resulting in enhanced production of free radicals thus causing oxidative stress<sup>4,23</sup>. As a result, selective MAO-B inhibitors are useful in neurodegenerative disorders such as AD.

Due to the complexity of AD, drugs that modulate the activity of a single target might not be sufficient to alter the progression of this disease. Thus, an efficient therapy is more likely to develop multi-targeted drugs that incorporate several pharmacological effects into a single molecule. Taking these facts into account, many researchers are devoted to the investigation of multi-target-directed ligand (MTDL)<sup>24</sup>,<sup>25</sup>. Subsequently, a variety of compounds combining the inhibitory activity of ChE, MAO and  $A\beta$  aggregation have been developed for the treatment of AD (Figure 1)<sup>26-31</sup>.

Coumarins are a large family of compounds from natural and synthetic origin that display a variety of biological properties, including *anti*-inflammatory and antioxidant properties<sup>32-36</sup>. Many researches have paid special attentions to its effects against AD, and a lot of reports also indicated that numerous functionalized coumarins can inhibit

$A\beta$  self-aggregation, attenuate  $A\beta$ -induced toxicity, promote  $A\beta$  clearance and reduce senile plaques<sup>37, 38</sup>. Several studies have been also reported that 3-arylcoumarins exhibited potent inhibitory effects on MAO and 3-(piperazine-1-carbonyl) coumarins showed significant AChE inhibitory activities<sup>39</sup>. With these reports in mind, it could be concluded that the 3-arylcoumarins might be privileged leading compounds in the design of multipotent ChE and MAO inhibitors for the treatment of AD.

Recently, we have reported the synthesis and evaluation of 6-methylcoumarins as selective MAO-B inhibitors<sup>40</sup>. Continuing with the previous work, in this paper we focused on designing novel multifunctional agents based on 6-methylcoumarin scaffolds for AD treatment. As known, coumarin moiety could interact with the PAS of AChE via aromatic stacking interactions and inhibit  $A\beta$  self-aggregation<sup>26</sup>. Since the AChE-CAS is located at the bottom of a deep gorge, we considered introducing variable amine side chains to connect with 3-arylcoumarins. These flexible linkers could be stayed by the enzyme cavity, allowing simultaneous interaction between the heteroaromatic fragments and both the PAS and CAS of AChE<sup>41</sup>. Consequently, a series of 3-arylcoumarin analogues linked with different amine groups by 2- to 5-carbon spacer were designed. In order to diversify the structures and investigate possible SAR, we also introduced some different small substituents in position 6 of the coumarin, and change the position of amine chains on the phenyl ring (*o*-, *m*-, *p*-) in 3-position of the coumarin ring (Figure 2).

Accordingly, in this work we describe the design, synthesis, biological evaluation and molecular modeling of 6-substituted 3-arylcoumarin derivatives as selective

AChE/MAO-B dual inhibitors. The pharmacological profiles of these new compounds including AChE and BuChE inhibition, MAO-A and MAO-B inhibition, self-induced  $A\beta_{42}$  aggregation, the kinetics of enzyme inhibition, antioxidant, blood-brain barrier permeation and neuroprotective effects were evaluated. Finally, molecular modeling studies were performed to gain insight into the binding mode and structure-activity relationships of the selected compounds.

## 2. Results and discussion

### 2.1. Chemistry

The synthetic routes of 6-substituted 3-arylcoumarin derivatives were shown in Scheme 1. The key intermediates **3a-e** were obtained by a minor modification according to the reported method <sup>24</sup>. By condensation of 5-substituted salicylaldehydes **1a-c** and the appropriate hydroxyphenylacetic derivatives **2a-c** with *N,N*-dicyclohexylcarbodiimide (DCC) as a coupling agent, the 3-arylcoumarin derivatives **3a-e** were synthesized via the classical Perkin reaction with moderate yields. The reaction of **3a-e** with different  $\alpha, \omega$ -dibromoalkanes in acetonitrile produced compounds **4a-h**. These compounds were then treated with dimethylamine and other secondary amines in the presence of potassium carbonate to afford the target products **5a-t** in 73-89% yields.

### 2.2. Pharmacological evaluation

#### 2.2.1. Cholinesterase inhibitory activity and SAR discussion

Inhibitory activities of the target compounds on AChE (from electric eel) and BuChE (from equine serum) were tested by the spectrophotometric method of Ellman

*et al.* with tacrine and galanthamine as reference standards<sup>42</sup>. The IC<sub>50</sub> values for eeAChE and eqBuChE inhibitions are summarized in Table 1. It could be seen from Table 1 that most of the synthesized compounds showed good inhibitory activities to ChEs with IC<sub>50</sub> values ranging from micromolar to nanomolar. All of the target compounds showed higher inhibitory potency against ChEs than the precursors **3c-e** and **1**, indicating that the introduction of amino group side chains could increase the inhibitory capacity of the target compounds. To get the optimal linker length, compounds **5a-d** were designed and synthesized. As shown in Table 1, compound **5a** was the best inhibitor against eeAChE (IC<sub>50</sub> = 2.81 μM) and eqBuChE (IC<sub>50</sub> = 1.93 μM), revealing that a two-carbon linker between the 6-substituted 3-aryl coumarin moiety and amine group was the suitable length for ChEs inhibition. When the optimal linker length was obtained, different terminal amine groups were introduced to explore structure-activity relationship. It is worth noting that **5a** and **5h** (**5h**, eeAChE IC<sub>50</sub> = 2.10 μM; eqBuChE IC<sub>50</sub> = 2.12 μM) were more potent than those with large amine groups (**5e-g**, **5i-k**). It could be concluded that small amine groups could increase eeAChE inhibitory potency but have no significant effect to eqBuChE. However, it was found that both eeAChE and eqBuChE inhibitory activities of compound **5j** with morpholine heterocyclic were decreased, which indicated that increased hydrophilic property could lead to a decrease in ChEs inhibitory potency. Moreover, compounds **5a**, **5h** and **5k** (**5k**, eeAChE IC<sub>50</sub> = 3.12 μM; eqBuChE IC<sub>50</sub> = 1.63 μM) behaved similarly in the inhibition to both eeAChE and eqBuChE, revealing that the modification of amino groups could not remarkably affect the inhibitory

potency.

In order to further improve the activity of the designed compounds against ChEs, we changed the substitution positions of amine side chains on the phenyl ring (*o*-, *m*-, *p*-) in 3-position of the coumarin. Among the compounds **5a**, **5h** (*m*-substituted), **5l-m** (*o*-substituted) and **5n-o** (*p*-substituted), the eeAChE inhibitory activities of *o*-substituted compounds were the lowest, and *p*-substituted compounds (**5n** IC<sub>50</sub> = 1.26 μM; **5o** IC<sub>50</sub> = 0.941 μM) exhibited slightly better inhibitory activities against eeAChE than *m*-substituted compounds (**5a** IC<sub>50</sub> = 2.81 μM; **5h** IC<sub>50</sub> = 2.10 μM). Interestingly, there was no clear trend for eqBuChE inhibitory activities. In addition, a methoxy group or a chlorine atom was introduced to the 6-position of the coumarin moiety to produce **5p-t**, which resulted in a slight increase in eeAChE inhibition but a significant decrease in eqBuChE inhibition. The results (**5p**, SI = 52.1; **5s**, SI = 85.0) suggested that the methoxy- or chloro-substituent could enhanced the selectivity of inhibitory activity for eeAChE.

Finally, some potential lead compounds (**5a**, **5h**, **5o-q**, **5s-t**) and the reference compound tacrine were then evaluated as inhibitors of human ChEs (hChEs)<sup>41</sup>. The IC<sub>50</sub> values of test compounds for human AChE (hAChE) and human BuChE (hBuChE) inhibition were summarized in Table 2. With exception of **5a**, **5h** and **5t**, all the tested derivatives showed nanomolar inhibition against hAChE and they were more potent as inhibitors of the human enzyme than that of the animal enzyme. The best hAChE inhibitor was **5q** and its inhibitory activity (IC<sub>50</sub> = 65 nM) was about 11 times than that of eeAChE (IC<sub>50</sub> = 713 nM). However, to our surprise, these

compounds revealed very poor inhibition for hBuChE ( $IC_{50} > 20 \mu\text{M}$ ). This phenomenon probably due to the conformational difference between hAChE and eeAChE<sup>43</sup>.

### 2.2.2. Kinetic study of hAChE inhibition

In order to gain insight into the mechanism of action of these derivatives on hAChE, compound **5p** was selected for kinetic measurements because it showed a good inhibitory activity against hAChE. The graphical analysis of the steady-state inhibition data of **5p** for hAChE was shown in Figure 3. The results indicated that both slopes and intercepts were increased at increasing concentration of the inhibitor. This pattern indicated that compound **5p** was a mixed-type inhibitor binding to the PAS as well as the CAS of hAChE, demonstrating rationality of our molecular design strategy.

### 2.2.3. Molecular modeling studies

To further investigate the binding mode of the inhibitors, the molecular docking study was performed with the more promising compound **5p** (**5o**, see Figure S1, Supporting Information) by using Molecular Operating Environment (MOE) software package. A mixed-type inhibition by **5p** was shown in the Lineweaver-Burk plot for hAChE, meaning that the binding sites might be the CAS as well as the PAS. Based on this, the X-ray crystal structure of hAChE in complex with dual binding sites inhibitor donepezil (PDB 4EY7) was chosen from the Protein Data Bank (<http://www.rcsb.org>). The protonation level of compound **5p** in physiological pH (7.4) was calculated by the Marvin software package (Version 14.12.8 2014),

ChemAxon (<http://www.chemaxon.com>). Since the amino groups of the ligands were protonated at physiologic pH, the ligands were recognized by the anionic subsite of the enzyme. It was reported that the feature of molecules takes part in recognition and orientation of the ligands towards the active site <sup>44</sup>.

By analyzing Figure 4, compound **5p** could perfectly fit into the active-site gorge of hAChE and simultaneously interact with the PAS and CAS of hAChE. The phenyl ring of coumarin was observed to bind to the PAS via  $\pi$ - $\pi$  stacking interactions with the indole ring of Trp 286. The 3-substituted phenyl ring was also bound to the PAS of hAChE, and stacked against the phenyl ring of Tyr 341. In the bottom of the gorge, the charged nitrogen of *N*-dimethylamino could bind to CAS by establishing a cation- $\pi$  interaction with the indole ring of Trp 86. The docking results revealed that the designed compound **5p** could bind to PAS and CAS dual binding sites, indicating a mixed-type inhibitor of hAChE, which were in agreement with kinetic analysis result.

#### 2.2.4. Inhibition of self-induced $A\beta_{42}$ aggregation

The inhibition of self-induced  $A\beta_{42}$  aggregation of these 6-substituted 3-arylcoumarin derivatives was evaluated using a Thioflavin-T based fluorometric assay <sup>45,46</sup>. Inhibition activities as inhibition ratios at a test concentration of 20  $\mu$ M were listed in Table 1. Compared with the reference compounds, resveratrol (66%, at 20  $\mu$ M) and curcumin (53%, at 20  $\mu$ M), compounds **5a-t**, **3c-e** and **1** gave different results with inhibition ratios from 21% to 85%. Compound **5s** was the strongest inhibitor among all the compounds. From the inhibition values, it was observed that

most of these compounds with amine side chains had better inhibitory activities than the precursors. Moreover, amine side chains on the *p*-position of phenyl ring (**5l-m**) led to a significant decrease in inhibitory activity of  $A\beta_{42}$  aggregation. Compounds **5s-t** exhibited higher levels of inhibitory potency than other compounds, revealing that an electron-withdrawing chloro-substituent on 6-position of the coumarins might be beneficial to their activities against self-induced  $A\beta_{42}$  aggregation.

#### 2.2.5. MAO inhibitory activity

Compounds **5a-t**, **3c-e** and **1** were also evaluated the activities of inhibiting the human MAOs<sup>40</sup>. The inhibitory activities were investigated by measuring the effects of each derivative on the production of hydrogen peroxide from *p*-tyramine, using the Amplex Red MAO assay, with chlorgyline, selegiline and iproniazid as references<sup>47</sup>. It could be seen from Table 3 that all the tested compounds showed greatly better inhibitory activities towards hMAO-B than hMAO-A. Some of them exhibited inhibition of hMAO-B equal or better than both the precursors (**3c-e** and **1**) and reference compound iproniazid. Among these compounds, **5a-b**, **5n-q** and **5s** exhibited good hMAO-B inhibitory activities in nanomolar ranges, which indicated that the substitution positions of amine side chains on the phenyl ring might be important for the hMAO-B activity and selectivity. The introduction of amino groups in *p*-position of the 3-phenyl ring increased the activity of hMAO-B, but the substitutions at *o*-position seem to be unfavorable for the activity (**5l-m**). The best hAChE inhibitor **5q** (hMAO-A,  $IC_{50} = 51.9 \mu\text{M}$ ; hMAO-B,  $IC_{50} = 758 \text{ nM}$ ) did not displayed more effective inhibition against MAOs. However, compounds **5o** and **5p**

exhibiting higher hMAO-B inhibitory activities, stronger inhibition of hAChE and significant inhibition of  $A\beta_{42}$  aggregation, showed balanced properties against both hAChE, hMAO-B and  $A\beta_{42}$ .

#### 2.2.6. Reversibility and kinetic studies of hMAO-B inhibition

To evaluate whether target compounds are reversible or irreversible hMAO-B inhibitors, the time-dependent inhibition assay was examined<sup>48</sup>. Compound **5p** was selected as a representative inhibitor since it was a potential hAChE/hMAO-B dual inhibitor with a stronger hMAO-B inhibitory activity. Compound **5p** was pre-incubated with hMAO-B over different time periods (0, 15, 30, 60 min) at a concentration of 400 nM. Data shown in Figure 5 indicated that **5p** was a reversible hMAO-B inhibitor because of a slightly time-dependent increase in hMAO-B activity.

Compound **5p** was also used to further investigate the mode of hMAO-B inhibition. The type of hMAO-B inhibition was determined by Michaelis-Menten kinetic experiments. The catalytic rates were measured at five different *p*-tyramine concentrations (50-500  $\mu$ M), and each plot was constructed at four different concentrations of **5p** (0, 100, 200 and 400 nM). The overlaid reciprocal Lineweaver-Burk plots (Figure 6) showed that the plots for different concentrations of **5p** were linear and intersected at the *x*-axis. This pattern indicated that **5p** was a noncompetitive hMAO-B inhibitor, and these results further proved that 6-substituted 3-aryl coumarin derivatives were reversible hMAO-B inhibitors.

#### 2.2.7. Molecular modeling studies

In order to explore the interaction modes of the potential compound **5p** (**5o**, see

Figure S1, Supporting Information) with hMAO-B, docking studies were employed with Molecular Operating Environment (MOE) software package. The protonation level of the compound in physiological pH was calculated by the Marvin software package (Version 14.12.8 2014). Crystallographic structures of hMAO-B (PDB 2V61) were used to dock the derivatives under study<sup>40</sup>.

As shown in Figure 7, the coumarin moiety of **5p** was located in the well-known binding pocket of hMAO-B<sup>49, 50</sup>, in close proximity of the flavin adenine dinucleotide (FAD) cofactor, and a  $\pi$ - $\pi$  stacking interaction was seen between Tyr 398 and the phenyl ring of coumarin. Meanwhile, another  $\pi$ - $\pi$  stacking interaction was formed between the 3-substituted phenyl ring and residues Tyr326. Additionally, the amino side chain moiety and 3-substituted phenyl ring occupied the entrance cavity, which was a hydrophobic subpocket existing only in the hMAO-B isoform and constituted by Leu 171, Ile 199, Tyr 326, Ile 316, Phe 99, Pro 104. As disclosed above, this interaction may also explain the good hMAO-B inhibitory activity of compound **5p**. Therefore, the docking simulations further confirmed that **5p** was a reversible and noncompetitive hMAO-B inhibitor.

### 2.3. ABTS radical cation scavenging assay

Compounds **5a-5t** were tested for their antioxidant activities by using the ABTS method<sup>51</sup>. Trolox (a water-soluble vitamin E analog) was used as a reference standard. Their antioxidant activities were provided as a trolox equivalent, with their relative potency at 25  $\mu$ M compared with trolox. As shown in Table 3, compounds **5o**, **5p**, **5q** and **5r** had the ability to scavenge the ABTS radical with 0.81, 1.17, 0.92, 1.26 trolox

equivalents respectively. All of these selected compounds demonstrated moderate antioxidant activities, with values 0.27 to 1.26 times that of trolox. The most active compounds were observed for **5p-r** with a methoxy group in 6-position of the arylcoumarin ring. However, methyl and halogen groups on the ring of arylcoumarin were unfavorable to the ABTS radicals scavenging activity.

#### 2.4. Blood-brain barrier (BBB) penetration

Since Alzheimer's disease affects the central nervous system (CNS), the effectiveness of the target compounds greatly depends upon their blood-brain barrier (BBB) penetration capacities<sup>52</sup>. To evaluate the potential for these derivatives to cross the BBB, we used a parallel artificial membrane permeation assay for BBB (PAMPA-BBB), which was described by Di *et al*<sup>53</sup>. Assay validation was made by comparing experimental permeabilities of 11 commercial drugs with reported values (Table S2, Supporting Information). A plot of experimental data versus bibliographic values gave a good linear correlation,  $P_e(\text{exp.}) = 1.0999 P_e(\text{bibl.}) + 1.2648$  ( $R^2 = 0.9475$ ). From this equation and taking into account the limit established by Di *et al*. for blood-brain barrier permeation, we classified compounds as follows:

- (a) ' CNS + ' (high BBB permeation predicted):  $P_e (10^{-6} \text{ cm s}^{-1}) > 5.66$ .
- (b) ' CNS - ' (low BBB permeation predicted):  $P_e (10^{-6} \text{ cm s}^{-1}) < 3.46$ .
- (c) ' CNS +/- ' (BBB permeation uncertain):  $P_e (10^{-6} \text{ cm s}^{-1})$  from 3.46 to 5.66

Finally, six compounds (**5a**, **5h**, **5n**, **5o**, **5p** and **5q**) exhibited good activities against hAChE, hMAO-B and  $A\beta_{42}$  aggregation were chosen as the test compounds. The results summarized in Table 4 indicated that all of the selected compounds could

penetrate the BBB.

### 2.5. Cell viability and neuroprotection against $A\beta_{42}$ -induced cytotoxicity

On basis of the screening results above, compounds **5o** and **5p**, as the multifunctional dual inhibitors against hAChE, hMAO-B and  $A\beta_{42}$ , were selected to further examine the potential toxicity effect on the PC12 cells<sup>54</sup>. After exposing the cells to these compounds for 24 h, the cell viability was evaluated by the 3-(4,5-dimethylthiazol-2-yl)-2,5-diphenyltetrazolium (MTT) assay. As reported in Figure 8, the results indicated that **5o** and **5p** did not show significant effect on cell viability at 3.125-50  $\mu$ M, suggesting that **5o** and **5p** exhibited very low toxicity to PC12 cells.

The neuroprotective activity of compounds **5o** and **5p** against  $A\beta_{42}$ -induced cytotoxicity in PC12 cells was investigated, since this peptide was the most amyloidogenic isoform of  $A\beta_{42}$ <sup>55</sup>. Melatonin was used as the reference compound. Treatment of PC12 cells for 24 h with 20  $\mu$ M  $A\beta_{42}$  caused cell viability to 56.8% compared to control. As shown in Figure 9, both the selected compounds and melatonin exhibited neuroprotective effects at concentrations ranging from 2.5 to 20  $\mu$ M, with compound **5p** showing the higher protective capability at 10  $\mu$ M. And the protective action against the  $A\beta_{42}$  peptide of our synthetic compounds might be enhanced by the anti- $A\beta_{42}$  aggregation action. Thus, **5o** and **5p** might be promising drug candidates for treating AD.

### 3. Conclusions

In conclusion, a series of 6-substituted 3-arylcoumarin derivatives were designed, synthesized and evaluated as multitarget-directed *anti*-Alzheimer agents for their

inhibitory activities on ChEs, MAOs, and  $A\beta_{42}$  aggregation. According to our screening results, most of those compounds could effectively and selectively inhibit hAChE and hMAO-B. Enzyme kinetic and the molecular modeling studies revealed the compounds could bind simultaneously to the PAS and CAS of AChE, as well as occupy the substrate binding site in hMAO-B. Compounds **5o** and **5p** also exhibited inhibitory percentages similar to the reference compounds resveratrol and curcumin in inhibition of  $A\beta_{42}$  self-aggregation assay. Besides, these compounds behaved good antioxidant, brain penetration capacity for CNS activity. In the cell viability and neuroprotection assay, **5o** and **5p** showed very low toxicity in PC12 cells and significant protective action against the  $A\beta_{42}$  peptide-induced cytotoxicity. Altogether, the multifunctional effects of these 6-substituted 3-arylcoumarin derivatives qualified them as potential anti-AD agents, and **5o** and **5p** might be promising drug candidates for further research.

#### **4. Experimental section**

##### *4.1. Chemistry. General methods*

All common reagents and solvents were obtained from commercial suppliers and used without further purification. Reaction progress was monitored using analytical thin layer chromatography (TLC) on precoated silica gel GF<sub>254</sub> plates (Qingdao Haiyang Chemical Plant, Qingdao, China) plates and the spots were detected under UV light (254 nm). Column chromatography was performed on silica gel (90-150  $\mu\text{m}$ ; Qingdao Marine Chemical Inc.) IR (KBr discs) spectra were recorded on a Bruker Tensor 27 spectrometer (Bruker, Karlsruhe, Germany). Melting point was measured

on an XT-4 micromelting point instrument and uncorrected.  $^1\text{H}$  NMR and  $^{13}\text{C}$  NMR spectra were measured on a Bruker ACF-500 spectrometer at 25 °C and referenced to TMS. Chemical shifts are reported in ppm ( $\delta$ ) using the residual solvent line as internal standard. The purity of all compounds used for biological evaluation was confirmed to be higher than 95% through analytical HPLC performed with Agilent 1200 HPLC System. A Zorbax SB-C<sub>18</sub> column (4.6 mm  $\times$  250 mm, 5  $\mu\text{m}$ , Agilent, Inc.) was used. The mobile phase was water (A) and MeOH (B) gradient system and the flow rate was 1.0 mL/min with 65% MeOH. Mass spectra were obtained on a MS Agilent 1100 Series LC/MSD Trap mass spectrometer (ESI-MS) and a Mariner ESI-TOF spectrometer (HRESI-MS), respectively.

#### 4.1.1. General procedures for the preparation of **3a-e**

A solution of 2-hydroxy-5-methylbenzaldehyde/2-hydroxy-5-methoxybenzaldehyde/2-hydroxy-5-chlorobenzaldehyde (**1a-c**) (8.0 mmol) and the corresponding substituted phenylacetic acid (**2a-c**) (10.0 mmol) in dimethyl sulfoxide (15 mL) was prepared. N, N'-Dicyclohexylcarbodiimide (11.4 mmol) was added, and the mixture was heated in an oil bath at 110 °C and stirred for 24-48 h. Ice (100 mL) and acetic acid (10 mL) were added to the reaction mixture. After keeping it at room temperature for 2 h, the mixture was extracted with ethyl acetate (3  $\times$  25 mL). The organic layer was extracted with sodium bicarbonate solution (50 mL, 5%) and then water (20 mL). The solvent was evaporated under vacuum, and the dry residue was purified by gel chromatography (petroleum/ethyl acetate 5:1)<sup>23</sup>.

##### 4.1.1.1.3-(2-Hydroxyphenyl)-6-methylcoumarin (**3a**)

Yield 75% (1.53 g), yellow solid;  $^1\text{H}$  NMR (500 MHz, DMSO)  $\delta$  9.58 (s, 1H), 7.98 (s, 1H), 7.55 (br s, 1H), 7.45 (dd,  $J = 8.5, 2.0$  Hz, 1H), 7.35 (d,  $J = 8.5$  Hz, 1H), 7.30-7.22 (m, 2H), 6.93 (d,  $J = 8.5$  Hz, 1H), 6.90-6.86 (m, 1H), 2.40 (s, 3H); MS (ESI)  $m/z$  253.1  $[\text{M}+\text{H}]^+$ .

#### 4.1.1.2.3-(3-Hydroxyphenyl)-6-methylcoumarin (**3b**)

Yield 68% (1.39 g), yellow solid;  $^1\text{H}$  NMR (500 MHz, DMSO)  $\delta$  9.56 (s, 1H), 8.15 (s, 1H), 7.59 (br s, 1H), 7.45 (dd,  $J = 8.5, 1.5$  Hz, 1H), 7.35 (d,  $J = 8.5$  Hz, 1H), 7.27 (t,  $J = 7.9$  Hz, 1H), 7.19-7.16 (m, 1H), 7.14 (d,  $J = 7.5$  Hz, 1H), 6.84 (dd,  $J = 8.5, 1.5$  Hz, 1H), 2.40 (s, 3H); MS (ESI)  $m/z$  253.1  $[\text{M}+\text{H}]^+$ .

#### 4.1.1.3.3-(4-Hydroxyphenyl)-6-methylcoumarin (**3c**)

Yield 72% (1.46 g), light yellow solid;  $^1\text{H}$  NMR (500 MHz, DMSO)  $\delta$  9.73 (s, 1H), 8.09 (s, 1H), 7.64-7.59 (m, 2H), 7.56 (d,  $J = 1.5$  Hz, 1H), 7.42 (dd,  $J = 8.5, 2.0$  Hz, 1H), 7.33 (d,  $J = 8.5$  Hz, 1H), 6.90-6.83 (m, 2H), 2.40 (s, 3H); MS (ESI)  $m/z$  253.1  $[\text{M}+\text{H}]^+$ .

#### 4.1.1.4.3-(4-hydroxyphenyl)-6-methoxy-2H-chromen-2-one (**3d**)

Yield 74% (1.51 g), yellow solid;  $^1\text{H}$  NMR (500 MHz, DMSO)  $\delta$  9.73 (s, 1H), 8.09 (s, 1H), 7.58 (d,  $J = 8.5$  Hz, 2H), 7.36 (d,  $J = 9.0$  Hz, 1H), 7.30 (d,  $J = 2.8$  Hz, 1H), 7.17 (dd,  $J = 9.0, 2.9$  Hz, 1H), 6.84 (d,  $J = 8.5$  Hz, 2H), 3.81 (s, 3H); MS (ESI)  $m/z$  269.1  $[\text{M}+\text{H}]^+$ .

#### 4.1.1.5.6-chloro-3-(4-hydroxyphenyl)-2H-chromen-2-one (**3e**)

Yield 75% (1.44 g), yellow solid;  $^1\text{H}$  NMR (500 MHz, DMSO)  $\delta$  9.81 (s, 1H), 8.10 (s, 1H), 7.85 (d,  $J = 2.5$  Hz, 1H), 7.63-7.56 (m, 3H), 7.45 (d,  $J = 8.8$  Hz, 1H), 6.85 (d,

$J = 8.7$  Hz, 2H); MS (ESI)  $m/z$  273.0  $[M+H]^+$ .

#### 4.1.2. General procedures for the preparation of **4a-h**

To a stirred mixture of appropriate amount of **3a-e** and  $K_2CO_3$  in acetonitrile, different available  $\alpha$ ,  $\omega$ -dibromoalkanes were added and the mixtures were heated at 50 °C for 6 h. After cooling to the room temperature, the mixture were filtered and the filtrates were evaporated under vacuum. The obtained residues were purified by silica gel chromatography with petroleum/ethyl acetate as eluent to give **4a-h**.

##### 4.1.2.1.3-(3-(2-bromoethoxy)phenyl)-6-methyl-2H-chromen-2-one (**4a**)

Yield 53% (0.95 g), light yellow solid;  $^1H$  NMR (500 MHz, DMSO)  $\delta$  8.23 (s, 1H), 7.57 (s, 1H), 7.45 (dd,  $J = 8.4, 1.9$  Hz, 1H), 7.39 (t,  $J = 7.8$  Hz, 1H), 7.36-7.30 (m, 3H), 7.09-6.98 (m, 1H), 4.38 (t,  $J = 5.7$  Hz, 2H), 3.84 (t,  $J = 5.3$  Hz, 2H), 2.39 (s, 3H); MS (ESI)  $m/z$  359.0  $[M+H]^+$ .

##### 4.1.2.2.3-(3-(3-bromopropoxy)phenyl)-6-methyl-2H-chromen-2-one (**4b**)

Yield 60% (0.26 g), yellow solid;  $^1H$  NMR (500 MHz, DMSO)  $\delta$  8.22 (s, 1H), 7.57 (s, 1H), 7.45 (dd,  $J = 8.4, 1.5$  Hz, 1H), 7.41-7.28 (m, 4H), 7.06-6.99 (m, 1H), 4.14 (t,  $J = 6.0$  Hz, 2H), 3.69 (t,  $J = 6.5$  Hz, 2H), 2.39 (s, 3H), 2.28 (p,  $J = 6.2$  Hz, 2H); MS (ESI)  $m/z$  373.0  $[M+H]^+$ .

##### 4.1.2.3.3-(3-(4-bromobutoxy)phenyl)-6-methyl-2H-chromen-2-one (**4c**)

Yield 63% (0.33 g), yellow solid;  $^1H$  NMR (500 MHz, DMSO)  $\delta$  8.22 (s, 1H), 7.57 (s, 1H), 7.45 (dd,  $J = 8.4, 1.5$  Hz, 1H), 7.41-7.28 (m, 4H), 7.06-6.99 (m, 1H), 4.14 (t,  $J = 6.0$  Hz, 2H), 3.69 (t,  $J = 6.5$  Hz, 2H), 2.39 (s, 3H), 2.01-1.96 (m, 4H); MS (ESI)  $m/z$  387.1  $[M+H]^+$ .

*4.1.2.4.3-(3-((5-bromopentyl)oxy)phenyl)-6-methyl-2H-chromen-2-one (4d)*

Yield 60% (0.38 g), yellow oil;  $^1\text{H NMR}$  (500 MHz, Acetone)  $\delta$  8.09 (s, 1H), 7.55 (s, 1H), 7.45 (dd,  $J = 8.4, 1.9$  Hz, 1H), 7.35 (tdd,  $J = 7.7, 5.3, 2.0$  Hz, 3H), 7.27 (d,  $J = 8.4$  Hz, 1H), 6.99 (ddd,  $J = 7.8, 2.4, 1.4$  Hz, 1H), 4.08 (t,  $J = 6.4$  Hz, 2H), 3.55 (t,  $J = 6.8$  Hz, 2H), 2.42 (s, 3H), 2.00-1.93 (m, 2H), 1.89-1.82 (m, 2H), 1.70-1.62 (m, 2H); MS (ESI)  $m/z$  401.1  $[\text{M}+\text{H}]^+$ .

*4.1.2.5.3-(2-(2-bromoethoxy)phenyl)-6-methyl-2H-chromen-2-one (4e)*

Yield 79% (0.24 g), yellow solid;  $^1\text{H NMR}$  (500 MHz, DMSO)  $\delta$  8.03 (s, 1H), 7.51 (s, 1H), 7.46-7.37 (m, 3H), 7.34 (d,  $J = 8.4$  Hz, 1H), 7.14 (d,  $J = 8.5$  Hz, 1H), 7.06 (t,  $J = 7.4$  Hz, 1H), 4.35 (t,  $J = 6.4$  Hz, 2H), 3.70 (t,  $J = 6.8$  Hz, 2H), 2.38 (s, 3H); MS (ESI)  $m/z$  359.0  $[\text{M}+\text{H}]^+$ .

*4.1.2.6.3-(4-(2-bromoethoxy)phenyl)-6-methyl-2H-chromen-2-one (4f)*

Yield 70% (0.43 g), light yellow solid;  $^1\text{H NMR}$  (500 MHz, DMSO)  $\delta$  8.13 (s, 1H), 7.70 (d,  $J = 8.7$  Hz, 2H), 7.55 (s, 1H), 7.42 (d,  $J = 8.4$  Hz, 1H), 7.32 (d,  $J = 8.4$  Hz, 1H), 7.08-7.04 (m, 2H), 4.39 (t,  $J = 5.7$  Hz, 2H), 3.83 (t,  $J = 6.1$  Hz, 2H), 2.38 (s, 3H); MS (ESI)  $m/z$  359.0  $[\text{M}+\text{H}]^+$ .

*4.1.2.7.3-(4-(2-bromoethoxy)phenyl)-6-methoxy-2H-chromen-2-one (4g)*

Yield 67% (0.71 g), yellow solid;  $^1\text{H NMR}$  (500 MHz, DMSO)  $\delta$  8.17 (s, 1H), 7.70 (d,  $J = 8.8$  Hz, 2H), 7.38 (d,  $J = 9.0$  Hz, 1H), 7.20 (dd,  $J = 9.0, 3.0$  Hz, 1H), 7.07 (d,  $J = 8.8$  Hz, 2H), 6.88 (d,  $J = 8.6$  Hz, 1H), 4.39 (t,  $J = 5.7$  Hz, 2H), 3.86-3.81 (m, 5H); MS (ESI)  $m/z$  375.0  $[\text{M}+\text{H}]^+$ .

*4.1.2.8.3-(4-(2-bromoethoxy)phenyl)-6-chloro-2H-chromen-2-one (4h)*

Yield 51% (0.57 g), yellow solid;  $^1\text{H}$  NMR (500 MHz, DMSO)  $\delta$  8.17 (s, 1H), 7.87 (d,  $J = 2.5$  Hz, 1H), 7.70 (d,  $J = 8.8$  Hz, 2H), 7.63-7.60 (m, 2H), 7.15 (d,  $J = 8.6$  Hz, 1H), 6.87 (d,  $J = 8.6$  Hz, 1H), 4.39 (t,  $J = 6.4$  Hz, 2H), 3.84 (t,  $J = 6.7$  Hz, 2H); MS (ESI)  $m/z$  379.5  $[\text{M}+\text{H}]^+$ .

#### 4.1.3. General procedures for the preparation of **5a-t**

To a stirred mixture of **4a-h** (0.2  $\mu\text{mol}$ ) and  $\text{K}_2\text{CO}_3$  (0.1 g, 0.7  $\mu\text{mol}$ ) in acetonitrile (5 mL), different available secondary amines (0.3 mmol) were added and the mixture was refluxed for 8 h. After cooling to the room temperature, the mixture was filtered and the filtrate was evaporated under vacuum. The obtained residues were purified by silica gel chromatography with  $\text{CH}_2\text{Cl}_2/\text{MeOH}$  as eluent to give target compounds

#### **5a-t.**

##### 4.1.3.1.3-(3-(2-(dimethylamino)ethoxy)phenyl)-6-methyl-2H-chromen-2-one (**5a**)

Yield 84% (56 mg), yellow solid; m.p. 93-95  $^\circ\text{C}$ ; IR (KBr)  $\nu$  3471, 2946, 2763, 1712, 1576, 1443, 1357, 1297, 1200, 1108, 1032  $\text{cm}^{-1}$ ;  $^1\text{H}$  NMR (500 MHz, DMSO)  $\delta$  8.22 (s, 1H), 7.57 (d,  $J = 1.0$  Hz, 1H), 7.44 (dd,  $J = 8.4, 1.8$  Hz, 1H), 7.39-7.32 (m, 2H), 7.31-7.28 (m, 2H), 7.00 (dd,  $J = 8.1, 1.6$  Hz, 1H), 4.10 (t,  $J = 5.8$  Hz, 2H), 2.65 (t,  $J = 5.7$  Hz, 2H), 2.38 (s, 3H), 2.23 (s, 6H);  $^{13}\text{C}$  NMR (125 MHz, DMSO)  $\delta$  160.19, 158.79, 151.63, 141.16, 136.50, 134.26, 133.12, 129.77, 128.76, 127.01, 121.31, 119.69, 116.11, 115.32, 115.06, 66.42, 58.19, 46.03, 46.03, 20.78; MS (ESI)  $m/z$  324.2  $[\text{M}+\text{H}]^+$ ; HRMS (ESI)  $m/z$  324.1596  $[\text{M}+\text{H}]^+$  (calcd for 324.1594,  $\text{C}_{20}\text{H}_{22}\text{NO}_3$ ).

##### 4.1.3.2.3-(3-(3-(dimethylamino)propoxy)phenyl)-6-methyl-2H-chromen-2-one (**5b**)

Yield 82% (57 mg), yellow solid; m.p. 93-95  $^\circ\text{C}$ ; IR (KBr)  $\nu$  3413, 2977, 2936,

2809, 2748, 1713, 1578, 1485, 1460, 1386, 1353, 1324, 1299, 1221, 1196, 1100, 1079, 1033, 927, 789  $\text{cm}^{-1}$ ;  $^1\text{H}$  NMR (500 MHz, DMSO)  $\delta$  8.21 (s, 1H), 7.57 (s, 1H), 7.44 (dd,  $J = 8.4, 1.7$  Hz, 1H), 7.38-7.32 (m, 2H), 7.28 (dd,  $J = 4.3, 2.3$  Hz, 2H), 6.98 (dd,  $J = 8.2, 1.7$  Hz, 1H), 4.04 (t,  $J = 6.4$  Hz, 2H), 2.40-2.34 (m, 5H), 2.15 (s, 6H), 1.90-1.83 (m, 2H);  $^{13}\text{C}$  NMR (125 MHz, DMSO- $d_6$ )  $\delta$  160.21, 158.95, 151.64, 141.14, 136.50, 134.26, 133.11, 129.77, 128.77, 127.05, 121.23, 119.70, 116.11, 115.27, 115.09, 66.42, 56.19, 45.69, 27.43, 20.78. MS (ESI)  $m/z$  338.2  $[\text{M}+\text{H}]^+$ ; HRMS (ESI)  $m/z$  338.1748  $[\text{M}+\text{H}]^+$  (calcd for 338.1751,  $\text{C}_{21}\text{H}_{24}\text{NO}_3$ ).

#### 4.1.3.3.3-(3-(4-(dimethylamino)butoxy)phenyl)-6-methyl-2H-chromen-2-one (5c)

Yield 73% (53 mg), colorless solid; m.p. > 250  $^\circ\text{C}$ ; IR (KBr)  $\nu$  3436, 2944, 2863, 2779, 1713, 1577, 1444, 1357, 1297, 1199, 1110, 1061, 975, 825, 790, 712, 691  $\text{cm}^{-1}$ ;  $^1\text{H}$  NMR (500 MHz, DMSO)  $\delta$  8.23 (s, 1H), 7.59 (s, 1H), 7.47 (dd,  $J = 8.4, 1.6$  Hz, 1H), 7.40-7.34 (m, 2H), 7.32-7.29 (m, 2H), 7.01 (dd,  $J = 8.2, 1.6$  Hz, 1H), 4.05 (t,  $J = 6.5$  Hz, 2H), 2.41 (s, 3H), 2.27 (t,  $J = 7.2$  Hz, 2H), 2.15 (s, 6H), 1.80-1.72 (m, 2H), 1.61-1.55 (m, 2H);  $^{13}\text{C}$  NMR (125 MHz, DMSO)  $\delta$  160.18, 158.94, 151.61, 141.11, 136.48, 134.25, 133.10, 129.74, 128.75, 127.04, 121.19, 119.68, 116.09, 115.31, 115.06, 67.95, 59.19, 45.61, 27.07, 24.05, 20.77; MS (ESI)  $m/z$  352.2  $[\text{M}+\text{H}]^+$ ; HRMS (ESI)  $m/z$  352.1904  $[\text{M}+\text{H}]^+$  (calcd for 352.1907,  $\text{C}_{22}\text{H}_{26}\text{NO}_3$ ).

#### 4.1.3.4.3-(3-((5-(dimethylamino)pentyl)oxy)phenyl)-6-methyl-2H-chromen-2-one (5d)

Yield 77% (58 mg), red oil; IR (KBr)  $\nu$  3432, 2932, 2868, 1721, 1580, 1467, 1384, 1298, 1199, 1109, 1036, 973, 911, 818, 691  $\text{cm}^{-1}$ ;  $^1\text{H}$  NMR (500 MHz, DMSO)  $\delta$  8.21 (s, 1H), 7.57 (s, 1H), 7.45 (d,  $J = 8.4$  Hz, 1H), 7.35 (dd,  $J = 15.5, 8.1$  Hz, 2H), 7.28

(dd,  $J = 4.4, 1.9$  Hz, 2H), 7.01-6.96 (m, 1H), 4.01 (t,  $J = 6.4$  Hz, 2H), 2.39-2.33 (m, 5H), 2.22 (s, 6H), 1.75 (dt,  $J = 13.4, 6.6$  Hz, 2H), 1.49 (dd,  $J = 14.7, 7.3$  Hz, 2H), 1.46-1.41 (m, 2H);  $^{13}\text{C}$  NMR (125 MHz, DMSO)  $\delta$  160.20, 158.64, 151.64, 141.20, 134.28, 133.14, 129.84, 128.77, 126.97, 121.54, 121.20, 119.68, 116.12, 115.37, 115.13, 65.93, 65.24, 57.84, 57.84, 32.66, 32.38, 31.70, 20.78; MS (ESI)  $m/z$  366.2 [M+H]<sup>+</sup>; HRMS (ESI)  $m/z$  366.2062 [M+H]<sup>+</sup> (calcd for 366.2064, C<sub>23</sub>H<sub>28</sub>NO<sub>3</sub>).

#### 4.1.3.5.3-(3-(2-(diethylamino)ethoxy)phenyl)-6-methyl-2H-chromen-2-one (5e)

Yield 81% (64 mg), yellow solid; m.p. 76-78 °C; IR (KBr)  $\nu$  3413, 2965, 2941, 2816, 1715, 1607, 1578, 1488, 1447, 1299, 1202, 1100, 1090, 1055, 982, 691 cm<sup>-1</sup>;  $^1\text{H}$  NMR (500 MHz, DMSO)  $\delta$  8.21 (s, 1H), 7.56 (s, 1H), 7.44 (d,  $J = 8.4$  Hz, 1H), 7.35 (dd,  $J = 17.2, 8.7$  Hz, 2H), 7.28 (dd,  $J = 4.2, 2.1$  Hz, 2H), 7.02-6.95 (m, 1H), 4.06 (t,  $J = 6.1$  Hz, 2H), 2.79 (t,  $J = 6.1$  Hz, 2H), 2.56 (q,  $J = 7.1$  Hz, 4H), 2.38 (s, 3H), 0.98 (t,  $J = 7.1$  Hz, 6H);  $^{13}\text{C}$  NMR (125 MHz, DMSO)  $\delta$  160.20, 158.83, 151.62, 141.13, 136.48, 134.26, 133.11, 129.75, 128.76, 127.01, 121.27, 119.67, 116.10, 115.26, 115.11, 66.97, 51.89, 47.52, 47.52, 20.77, 12.37, 12.37. MS (ESI)  $m/z$  352.2 [M+H]<sup>+</sup>; HRMS (ESI)  $m/z$  352.1908 [M+H]<sup>+</sup> (calcd for 352.1907, C<sub>22</sub>H<sub>26</sub>NO<sub>3</sub>).

#### 4.1.3.6.3-(3-(2-(dipropylamino)ethoxy)phenyl)-6-methyl-2H-chromen-2-one (5f)

Yield 76% (68 mg), yellow oil; IR (KBr)  $\nu$  3435, 2959, 2872, 1724, 1580, 1491, 1442, 1353, 1299, 1255, 1198, 1107, 1051, 980, 816, 689 cm<sup>-1</sup>;  $^1\text{H}$  NMR (500 MHz, DMSO)  $\delta$  8.20 (s, 1H), 7.57 (s, 1H), 7.44 (d,  $J = 8.4$  Hz, 1H), 7.39-7.32 (m, 2H), 7.29 (s, 2H), 6.99 (d,  $J = 7.8$  Hz, 1H), 4.11 (t,  $J = 5.7$  Hz, 2H), 2.85 (t,  $J = 5.7$  Hz, 2H), 2.54 (t,  $J = 7.3$  Hz, 4H), 2.38 (s, 3H), 1.46-1.35(m, 4H), 0.85 (t,  $J = 7.3$  Hz, 6H);  $^{13}\text{C}$

NMR (125 MHz, DMSO-d<sub>6</sub>)  $\delta$  160.21, 158.65, 151.63, 141.15, 136.52, 134.29, 133.14, 129.80, 128.76, 127.00, 121.40, 119.66, 116.10, 115.29, 115.15, 66.32, 56.39, 56.39, 52.81, 20.76, 20.76, 19.99, 12.04, 12.04. MS (ESI)  $m/z$  380.2 [M+H]<sup>+</sup>; HRMS (ESI)  $m/z$  380.2219 [M+H]<sup>+</sup> (calcd for 380.2220, C<sub>24</sub>H<sub>30</sub>NO<sub>3</sub>).

*4.1.3.7.3-(3-(2-(dibutylamino)ethoxy)phenyl)-6-methyl-2H-chromen-2-one (5g)*

Yield 78% (70 mg), yellow oil; IR (KBr)  $\nu$  3435, 2957, 2930, 2870, 1726, 1580, 1491, 1442, 1353, 1298, 1254, 1197, 1134, 1106, 1043, 979, 931, 789, 689 cm<sup>-1</sup>; <sup>1</sup>H NMR (500 MHz, DMSO)  $\delta$  8.20 (s, 1H), 7.56 (s, 1H), 7.43 (t,  $J$  = 10.6 Hz, 1H), 7.39-7.31 (m, 2H), 7.31-7.22 (m, 2H), 6.98 (d,  $J$  = 8.2 Hz, 1H), 4.12 (t,  $J$  = 7.6 Hz, 2H), 3.34 (s, 4H), 2.86 (t,  $J$  = 8.2 Hz, 2H), 2.38 (s, 3H), 1.37 (dd,  $J$  = 25.5, 5.6 Hz, 4H), 1.32-1.25 (m, 4H), 0.86 (t,  $J$  = 7.3 Hz, 6H); <sup>13</sup>C NMR (125 MHz, DMSO)  $\delta$  160.19, 158.73, 151.62, 141.12, 136.49, 134.27, 133.12, 129.78, 128.75, 127.02, 121.31, 119.66, 116.10, 115.24, 115.16, 54.24, 54.24, 52.85, 47.05, 29.27, 28.05, 20.76, 20.41, 20.41, 14.35, 14.35. MS (ESI)  $m/z$  408.3 [M+H]<sup>+</sup>; HRMS (ESI)  $m/z$  408.2532 [M+H]<sup>+</sup> (calcd for 408.2533, C<sub>26</sub>H<sub>34</sub>NO<sub>3</sub>).

*4.1.3.8.6-methyl-3-(3-(2-(pyrrolidin-1-yl)ethoxy)phenyl)-2H-chromen-2-one (5h)*

Yield 81% (59 mg), yellow oil; IR (KBr)  $\nu$  3448, 2924, 2775, 1712, 1604, 1577, 1486, 1441, 1354, 1296, 1198, 1105, 1050, 975, 789, 691 cm<sup>-1</sup>; <sup>1</sup>H NMR (500 MHz, DMSO)  $\delta$  8.21 (s, 1H), 7.56 (s, 1H), 7.44 (d,  $J$  = 8.4 Hz, 1H), 7.39-7.28 (m, 4H), 7.03-6.97 (m, 1H), 4.13 (t,  $J$  = 5.8 Hz, 2H), 2.88 (t,  $J$  = 6.2 Hz, 2H), 2.60 (s, 4H), 2.38 (s, 3H), 1.71 (s, 4H); <sup>13</sup>C NMR (125 MHz, DMSO)  $\delta$  160.19, 158.72, 151.62, 141.16, 136.51, 134.26, 133.12, 129.78, 128.76, 126.98, 121.36, 119.67, 116.10, 115.33,

115.07, 67.05, 54.69, 54.47, 54.47, 23.61, 23.61, 20.77. MS (ESI)  $m/z$  350.2 [M+H]<sup>+</sup>;  
HRMS (ESI)  $m/z$  350.1749 [M+H]<sup>+</sup> (calcd for 350.1751, C<sub>22</sub>H<sub>24</sub>NO<sub>3</sub>).

*4.1.3.9.6-methyl-3-(3-(2-(piperidin-1-yl)ethoxy)phenyl)-2H-chromen-2-one (5i)*

Yield 80% (60 mg), yellow solid; m.p. 110-112 °C; IR (KBr)  $\nu$  3446, 2930, 1712, 1578, 1488, 1442, 1355, 1299, 1170, 1107, 1052, 976, 875, 690 cm<sup>-1</sup>; <sup>1</sup>H NMR (500 MHz, DMSO)  $\delta$  8.22 (s, 1H), 7.56 (s, 1H), 7.44 (d,  $J$  = 8.3 Hz, 1H), 7.35 (dd,  $J$  = 15.2, 8.1 Hz, 2H), 7.29 (s, 2H), 7.00 (d,  $J$  = 8.1 Hz, 1H), 4.11 (t,  $J$  = 5.8 Hz, 2H), 2.67 (t,  $J$  = 5.8 Hz, 2H), 2.44 (s, 4H), 2.38 (s, 3H), 1.54-1.45 (m, 4H), 1.38 (d,  $J$  = 4.5 Hz, 2H); <sup>13</sup>C NMR (125 MHz, DMSO)  $\delta$  160.20, 158.81, 151.62, 141.15, 136.48, 134.26, 133.11, 129.75, 128.76, 127.01, 121.29, 119.68, 116.10, 115.30, 115.14, 66.24, 57.87, 54.92, 54.92, 26.08, 26.08, 24.42, 20.78. MS (ESI)  $m/z$  364.2 [M+H]<sup>+</sup>; HRMS (ESI)  $m/z$  364.1906 [M+H]<sup>+</sup> (calcd for 364.1907, C<sub>23</sub>H<sub>26</sub>NO<sub>3</sub>).

*4.1.3.10. 6-methyl-3-(3-(2-morpholinoethoxy)phenyl)-2H-chromen-2-one (5j)*

Yield 76% (57 mg), light yellow solid; m.p. 118-120 °C; IR (KBr)  $\nu$  3430, 2954, 1723, 1578, 1442, 1352, 1301, 1259, 1225, 1199, 1114, 1051, 970, 817, 711, 691 cm<sup>-1</sup>; <sup>1</sup>H NMR (500 MHz, DMSO)  $\delta$  8.22 (s, 1H), 7.56 (s, 1H), 7.44 (d,  $J$  = 7.9 Hz, 1H), 7.40-7.32 (m, 2H), 7.30 (d,  $J$  = 6.6 Hz, 2H), 7.01 (d,  $J$  = 7.4 Hz, 1H), 4.15 (t,  $J$  = 5.3 Hz, 2H), 3.59 (s, 4H), 3.33 (s, 4H), 2.75 (t,  $J$  = 5.7 Hz, 2H), 2.38 (s, 3H); <sup>13</sup>C NMR (125 MHz, DMSO)  $\delta$  160.20, 158.71, 151.62, 141.17, 136.50, 134.27, 133.13, 129.77, 128.76, 126.98, 121.39, 119.67, 116.11, 115.36, 115.13, 66.56, 63.83, 57.44, 54.05, 54.05, 20.77, 20.77. MS (ESI)  $m/z$  366.2 [M+H]<sup>+</sup>; HRMS (ESI)  $m/z$  366.1698 [M+H]<sup>+</sup> (calcd for 366.1700, C<sub>22</sub>H<sub>24</sub>NO<sub>4</sub>).

4.1.3.11. 3-(3-(2-(benzyl(methyl)amino)ethoxy)phenyl)-6-methyl-2H-chromen-2-one (5k)

Yield 76% (63 mg), yellow oil; IR (KBr)  $\nu$  3434, 3028, 2924, 2875, 2843, 1723, 1579, 1492, 1451, 1352, 1299, 1255, 1224, 1198, 1171, 1107, 1037, 979, 816, 699  $\text{cm}^{-1}$ ;  $^1\text{H}$  NMR (500 MHz, DMSO)  $\delta$  8.20 (s, 1H), 7.56 (s, 1H), 7.44 (d,  $J = 8.4$  Hz, 1H), 7.36-7.28 (m, 8H), 7.22 (dd,  $J = 8.8, 4.3$  Hz, 1H), 6.99 (dd,  $J = 8.1, 1.3$  Hz, 1H), 4.15 (t,  $J = 5.9$  Hz, 2H), 3.58 (s, 2H), 2.76 (t,  $J = 5.9$  Hz, 2H), 2.38 (s, 3H), 2.24 (s, 3H);  $^{13}\text{C}$  NMR (125 MHz, DMSO)  $\delta$  160.24, 158.75, 151.59, 141.16, 139.41, 136.47, 134.31, 133.14, 129.78, 129.21, 128.76, 128.76, 128.60, 128.60, 127.33, 127.00, 121.32, 119.64, 116.09, 115.28, 115.13, 66.53, 62.19, 55.73, 42.86, 20.76. MS (ESI)  $m/z$  400.2  $[\text{M}+\text{H}]^+$ ; HRMS (ESI)  $m/z$  400.1905  $[\text{M}+\text{H}]^+$  (calcd for 400.1907,  $\text{C}_{26}\text{H}_{26}\text{NO}_3$ ).

4.1.3.12. 3-(2-(2-(dimethylamino)ethoxy)phenyl)-6-methyl-2H-chromen-2-one (5l)

Yield 83% (56 mg), yellow solid; m.p. 55-57 °C; IR (KBr)  $\nu$  3424, 2927, 2820, 2771, 1722, 1578, 1493, 1450, 1354, 1279, 1242, 1167, 1128, 1098, 1037, 960, 818, 758  $\text{cm}^{-1}$ ;  $^1\text{H}$  NMR (500 MHz, DMSO)  $\delta$  7.99 (s, 1H), 7.49 (s, 1H), 7.43 (dd,  $J = 8.5, 1.7$  Hz, 1H), 7.41-7.31 (m, 3H), 7.12 (d,  $J = 8.2$  Hz, 1H), 7.01 (t,  $J = 7.4$  Hz, 1H), 4.06 (t,  $J = 5.8$  Hz, 2H), 2.52 (t,  $J = 5.8$  Hz, 2H), 2.37 (s, 3H), 2.11 (s, 6H);  $^{13}\text{C}$  NMR (125 MHz, DMSO)  $\delta$  160.10, 155.71, 151.88, 142.77, 134.30, 133.08, 131.49, 130.58, 128.57, 126.22, 124.94, 121.73, 119.40, 116.28, 112.94, 69.57, 62.10, 55.39, 49.94, 20.77. MS (ESI)  $m/z$  324.2  $[\text{M}+\text{H}]^+$ ; HRMS (ESI)  $m/z$  324.1592  $[\text{M}+\text{H}]^+$  (calcd for 324.1594,  $\text{C}_{20}\text{H}_{22}\text{NO}_3$ ).

4.1.3.13. 6-methyl-3-(2-(2-(pyrrolidin-1-yl)ethoxy)phenyl)-2H-chromen-2-one

(5m)

Yield 85% (62 mg), yellow solid; m.p. 62-64 °C; IR (KBr)  $\nu$  3430, 2924, 2786, 1725, 1580, 1492, 1451, 1352, 1249, 1167, 1126, 1098, 1029, 959, 817, 781, 756  $\text{cm}^{-1}$ ;  $^1\text{H}$  NMR (500 MHz, DMSO)  $\delta$  7.98 (s, 1H), 7.49 (s, 1H), 7.37 (ddd,  $J = 14.1, 13.1, 8.8$  Hz, 4H), 7.11 (d,  $J = 8.3$  Hz, 1H), 7.02 (t,  $J = 7.4$  Hz, 1H), 4.08 (t,  $J = 5.7$  Hz, 2H), 2.69 (t,  $J = 5.5$  Hz, 2H), 2.41 (s, 4H), 2.37 (s, 3H), 1.55 (s, 4H);  $^{13}\text{C}$  NMR (125 MHz, DMSO)  $\delta$  159.95, 156.75, 151.75, 142.47, 134.18, 132.87, 131.15, 130.47, 128.41, 126.04, 124.96, 120.86, 119.43, 116.19, 113.10, 68.07, 55.36, 54.49, 54.49, 23.56, 23.56, 20.75. MS (ESI)  $m/z$  350.2  $[\text{M}+\text{H}]^+$ ; HRMS (ESI)  $m/z$  350.1748  $[\text{M}+\text{H}]^+$  (calcd for 350.1751,  $\text{C}_{22}\text{H}_{24}\text{NO}_3$ ).

4.1.3.14. 3-(4-(2-(dimethylamino)ethoxy)phenyl)-6-methyl-2H-chromen-2-one

(5n)

Yield 73% (49 mg), yellow solid; m.p. 84-86 °C; IR (KBr)  $\nu$  3404, 2949, 2814, 2768, 1715, 1603, 1577, 1513, 1462, 1353, 1287, 1154, 1190, 1162, 1135, 1115, 1027, 966, 827, 781, 619  $\text{cm}^{-1}$ ;  $^1\text{H}$  NMR (500 MHz, DMSO)  $\delta$  8.12 (s, 1H), 7.85 (d,  $J = 8.7$  Hz, 1H), 7.68 (d,  $J = 8.7$  Hz, 2H), 7.54 (s, 1H), 7.32 (d,  $J = 8.4$  Hz, 1H), 7.03 (d,  $J = 8.8$  Hz, 2H), 4.10 (t,  $J = 5.8$  Hz, 2H), 2.64 (t,  $J = 6.2$  Hz, 2H), 2.37 (s, 3H), 2.23 (s, 6H);  $^{13}\text{C}$  NMR (125 MHz, DMSO)  $\delta$  160.45, 158.04, 151.46, 139.85, 134.25, 132.81, 132.22, 130.36, 128.58, 126.70, 119.82, 116.08, 115.75, 115.04, 69.80, 61.92, 55.39, 50.11, 50.11, 20.79. MS (ESI)  $m/z$  324.2  $[\text{M}+\text{H}]^+$ ; HRMS (ESI)  $m/z$  324.1595  $[\text{M}+\text{H}]^+$  (calcd for 324.1594,  $\text{C}_{20}\text{H}_{22}\text{NO}_3$ ).

4.1.3.15. *6-methyl-3-(4-(2-(pyrrolidin-1-yl)ethoxy)phenyl)-2H-chromen-2-one*

(5o)

Yield 77% (56 mg), yellow solid; m.p. 63-65 °C; IR (KBr)  $\nu$  3398, 2928, 2784, 1715, 1604, 1578, 1513, 1453, 1351, 1256, 1184, 1169, 1117, 1032, 963, 880, 781  $\text{cm}^{-1}$ ;  $^1\text{H}$  NMR (500 MHz, DMSO)  $\delta$  8.12 (s, 1H), 7.86 (d,  $J = 8.7$  Hz, 1H), 7.68 (d,  $J = 8.8$  Hz, 2H), 7.54 (s, 1H), 7.32 (d,  $J = 8.4$  Hz, 1H), 7.03 (d,  $J = 8.8$  Hz, 2H), 4.15 (t,  $J = 5.7$  Hz, 2H), 2.94-2.87 (m, 4H), 2.60 (t,  $J = 5.5$  Hz, 2H), 2.37 (s, 3H), 1.72 (s, 4H);  $^{13}\text{C}$  NMR (125 MHz, DMSO)  $\delta$  159.95, 156.75, 151.75, 142.47, 134.18, 132.87, 131.15, 130.47, 128.41, 126.04, 124.96, 120.86, 119.43, 116.19, 113.10, 68.07, 55.36, 54.49, 54.49, 23.56, 23.56, 20.75. MS (ESI)  $m/z$  350.2  $[\text{M}+\text{H}]^+$ ; HRMS (ESI)  $m/z$  350.1753  $[\text{M}+\text{H}]^+$  (calcd for 350.1751,  $\text{C}_{22}\text{H}_{24}\text{NO}_3$ ).

4.1.3.16. *3-(4-(2-(dimethylamino)ethoxy)phenyl)-6-methoxy-2H-chromen-2-one*

(5p)

Yield 81% (54 mg), yellow solid; m.p. 82-84 °C; IR (KBr)  $\nu$  3436, 2930, 2853, 2775, 1705, 1605, 1575, 1513, 1450, 1353, 1296, 1154, 1188, 1121, 1028, 965, 805, 701  $\text{cm}^{-1}$ ;  $^1\text{H}$  NMR (500 MHz, DMSO)  $\delta$  8.15 (s, 1H), 7.68 (d,  $J = 8.6$  Hz, 2H), 7.37 (d,  $J = 9.0$  Hz, 1H), 7.31 (d,  $J = 2.8$  Hz, 1H), 7.03 (d,  $J = 8.7$  Hz, 2H), 6.84 (d,  $J = 8.4$  Hz, 1H), 4.10 (t,  $J = 5.7$  Hz, 2H), 3.82 (s, 3H), 2.64 (t,  $J = 5.7$  Hz, 2H), 2.22 (s, 6H);  $^{13}\text{C}$  NMR (125 MHz, DMSO)  $\delta$  160.42, 158.07, 156.19, 147.71, 139.76, 130.36, 130.36, 128.41, 127.04, 120.54, 119.43, 117.38, 115.05, 115.05, 111.20, 69.81, 61.79, 56.23, 50.15, 50.15. MS (ESI)  $m/z$  340.2  $[\text{M}+\text{H}]^+$ ; HRMS (ESI)  $m/z$  340.1541  $[\text{M}+\text{H}]^+$  (calcd for 340.1543,  $\text{C}_{20}\text{H}_{22}\text{NO}_4$ ).

4.1.3.17. 6-methoxy-3-(4-(2-(pyrrolidin-1-yl)ethoxy)phenyl)-2H-chromen-2-one

(5q)

Yield 75% (54 mg), yellow solid; m.p. 50-52 °C; IR (KBr)  $\nu$  3431, 2930, 2853, 1705, 1609, 1575, 1513, 1450, 1352, 1296, 1255, 1188, 1122, 1029, 966, 881, 701  $\text{cm}^{-1}$ ;  $^1\text{H}$  NMR (500 MHz, DMSO)  $\delta$  8.17 (s, 1H), 7.70 (d,  $J$  = 8.8 Hz, 2H), 7.41-7.37 (m, 1H), 7.33 (d,  $J$  = 2.9 Hz, 1H), 7.05 (d,  $J$  = 8.8 Hz, 2H), 6.86 (d,  $J$  = 8.6 Hz, 1H), 4.14 (t,  $J$  = 5.9 Hz, 2H), 3.84 (s, 3H), 2.84 (t,  $J$  = 5.8 Hz, 2H), 2.55 (d,  $J$  = 5.8 Hz, 4H), 1.77 (dd,  $J$  = 12.7, 6.0 Hz, 4H);  $^{13}\text{C}$  NMR (125 MHz, DMSO)  $\delta$  160.43, 159.33, 156.17, 147.65, 139.44, 130.89, 130.29, 130.29, 127.42, 120.60, 119.28, 117.33, 114.76, 114.76, 111.14, 67.18, 56.20, 55.36, 55.36, 54.46, 23.64, 23.64. MS (ESI)  $m/z$  366.2  $[\text{M}+\text{H}]^+$ ; HRMS (ESI)  $m/z$  366.1699  $[\text{M}+\text{H}]^+$  (calcd for 366.1700,  $\text{C}_{22}\text{H}_{24}\text{NO}_4$ ).

4.1.3.18. 3-(4-(2-(benzyl(methyl)amino)ethoxy)phenyl)-6-methoxy-2H-chromen-2-one (5r)

Yield 76% (63 mg), yellow oil; IR (KBr)  $\nu$  3261, 3064, 2931, 2854, 1724, 1641, 1549, 1512, 1453, 1352, 1295, 1247, 1176, 1118, 1028, 960, 818, 737, 699  $\text{cm}^{-1}$ ;  $^1\text{H}$  NMR (500 MHz, DMSO)  $\delta$  8.15 (s, 1H), 7.87 (d,  $J$  = 7.8 Hz, 2H), 7.69-7.66 (m, 2H), 7.24 (dt,  $J$  = 8.6, 5.1 Hz, 5H), 7.18 (d,  $J$  = 2.7 Hz, 1H), 7.02 (t,  $J$  = 10.3 Hz, 2H), 4.15 (t,  $J$  = 5.8 Hz, 2H), 3.82 (s, 3H), 3.58 (s, 2H), 2.76 (t,  $J$  = 5.8 Hz, 2H), 2.24 (s, 3H);  $^{13}\text{C}$  NMR (125 MHz, DMSO)  $\delta$  160.24, 158.75, 151.59, 141.16, 139.41, 136.47, 134.31, 133.14, 129.78, 129.21, 128.76, 128.76, 128.60, 128.60, 127.33, 127.00, 121.32, 119.64, 116.09, 115.28, 115.13, 66.53, 62.19, 59.13, 55.73, 42.86. MS (ESI)  $m/z$  416.2  $[\text{M}+\text{H}]^+$ ; HRMS (ESI)  $m/z$  416.1855  $[\text{M}+\text{H}]^+$  (calcd for 416.1856,

C<sub>26</sub>H<sub>26</sub>NO<sub>4</sub>).

4.1.3.19. *6-chloro-3-(4-(2-(ethyl(methyl)amino)ethoxy)phenyl)-2H-chromen-2-one*  
(5s)

Yield 75% (50 mg), yellow solid; m.p. 180-182 °C; IR (KBr)  $\nu$  3330, 2928, 2852, 1721, 1615, 1513, 1451, 1246, 1181, 1122, 1078, 962, 814, 699 cm<sup>-1</sup>; <sup>1</sup>H NMR (500 MHz, DMSO)  $\delta$  8.15 (s, 1H), 7.88 (d,  $J$  = 8.7 Hz, 1H), 7.70 (d,  $J$  = 8.7 Hz, 2H), 7.56 (s, 1H), 7.43 (dd,  $J$  = 8.4, 1.4 Hz, 1H), 7.05 (d,  $J$  = 8.8 Hz, 2H), 4.12 (t,  $J$  = 5.8 Hz, 2H), 2.67 (t,  $J$  = 5.7 Hz, 2H), 2.25 (s, 6H); <sup>13</sup>C NMR (125 MHz, DMSO)  $\delta$  159.94, 158.79, 151.74, 137.58, 131.06, 130.37, 130.37, 128.68, 128.34, 127.73, 125.35, 121.64, 118.23, 115.63, 115.63, 69.80, 61.92, 50.11 50.11. MS (ESI)  $m/z$  344.1 [M+H]<sup>+</sup>; HRMS (ESI)  $m/z$  344.1045 [M+H]<sup>+</sup> (calcd for 344.1048, C<sub>19</sub>H<sub>19</sub>ClNO<sub>3</sub>).

4.1.3.20. *6-chloro-3-(4-(2-(pyrrolidin-1-yl)ethoxy)phenyl)-2H-chromen-2-one* (5t)

Yield 73% (53 mg), yellow solid; m.p. 96-98 °C; IR (KBr)  $\nu$  3331, 2926, 2851, 1722, 1607, 1512, 1451, 1245, 1174, 1113, 987, 815 cm<sup>-1</sup>; <sup>1</sup>H NMR (500 MHz, DMSO)  $\delta$  8.18 (s, 1H), 7.87 (d,  $J$  = 2.5 Hz, 1H), 7.71 (d,  $J$  = 8.7 Hz, 2H), 7.65 (dd,  $J$  = 8.9, 2.2 Hz, 1H), 7.49 (d,  $J$  = 8.8 Hz, 1H), 7.07 (d,  $J$  = 8.7 Hz, 2H), 4.17 (t,  $J$  = 5.7 Hz, 2H), 3.62-3.41 (m, 4H), 2.13 (t,  $J$  = 5.7 Hz, 2H), 1.56 (d,  $J$  = 12.3 Hz, 4H); <sup>13</sup>C NMR (125 MHz, DMSO)  $\delta$  159.94, 158.79, 151.74, 137.58, 131.06, 130.37, 130.37, 128.68, 128.34, 127.73, 125.35, 121.64, 118.23, 115.63, 115.63, 67.18, 55.36, 54.46, 54.46, 23.64, 23.64. MS (ESI)  $m/z$  370.1 [M+H]<sup>+</sup>; HRMS (ESI)  $m/z$  370.1207 [M+H]<sup>+</sup> (calcd for 370.1204, C<sub>21</sub>H<sub>21</sub>ClNO<sub>3</sub>).

4.2. *Pharmacology*

#### 4.2.1. *In vitro* inhibition of AChE and BuChE

Acetylcholinesterase (AChE, E.C. 3.1.1.7, from the electric eel and hAChE, E.C. 3.1.1.7, from human erythrocytes), butyrylcholinesterase (BuChE, E.C. 3.1.1.8, from equine serum and hBuChE, E.C. 3.1.1.8, from human serum), 5, 5'-dithiobis-(2-nitrobenzoic acid) (Ellman's reagent, DTNB), acetylthiocholine chloride (ATC), and butylthiocholine chloride (BTC) were purchased from Sigma-Aldrich. The capacity of the test compounds to inhibit AChE and BuChE activities was assessed by Ellman's method<sup>42</sup>. Test compounds were dissolved in a minimum volume of DMSO (1%) and were diluted using the buffer solution (50 mM Tris-HCl, pH = 8.0, 0.1 M NaCl, 0.02 M MgCl<sub>2</sub>·6H<sub>2</sub>O) to the final concentration. In 96-well plates, 160 µL of 1.5 mM DTNB and 50 µL of AChE (0.22 U/mL prepared in 50 mM Tris-HCl, pH = 8.0, 0.1% w/v bovine serum albumin (BSA)) or 50 µL of BuChE (0.12 U/mL prepared in 50 mM Tris-HCl, pH = 8.0, 0.1% w/v BSA) were incubated with 10 µL of various concentrations of test compounds (0.01-100 µM) at 37 °C for 5 min followed by the addition of 30 µL acetylthiocholine iodide (15 mM) or S-butyrylthiocholine iodide (15 mM) and the absorbance was measured at different time intervals (0, 60, 120 and 180 s) at a wavelength of 405 nm. The concentration of compound producing 50% of enzyme activity inhibition (IC<sub>50</sub>) was calculated by nonlinear regression analysis of the response-concentration (log) curve, using Graph-Pad Prism program package (Graph Pad Software; San Diego, CA). Calculations were performed according to the method of Ellman *et al.* Results are expressed as the mean ± SEM of at least three different experiments performed in triplicate.

#### 4.2.2. Kinetic characterization of hAChE inhibition

To obtain the mechanism of action of **5p**, reciprocal plots of  $1/\text{velocity}$  versus  $1/[\text{substrate}]$  were constructed at different concentrations of the substrate thiocholine iodide (0.05-0.5 mM) by using Ellman's method. Compound **5p** was added to the assay solution and pre-incubated with the enzyme at 37 °C for 15 min, followed by the addition of ATC. The assay solution (200  $\mu\text{L}$ ) containing compound **5p** (0.10, 0.20, 0.40  $\mu\text{M}$ ), DTNB (1.5 mM), 10  $\mu\text{L}$  hAChE and ATCI (0.05, 0.075, 0.1, 0.15, 0.2, 0.5 mM) was dissolved in 0.1 M  $\text{KH}_2\text{PO}_4/\text{K}_2\text{HPO}_4$  buffer (pH 8.0). Kinetic characterization of the hydrolysis of acetylthiocholine catalyzed by hAChE was done spectrometrically at 405 nm. A parallel control experiment was carried out without compound **5p** in the mixture. Slopes of these reciprocal plots were then plotted against the concentration of **5p** in a weighted analysis and  $K_i$  was determined as the intercept on the negative  $x$ -axis. Data analysis was performed with GraphPad Prism 4.03 software (GraphPad Software Inc.).

#### 4.2.3. Inhibition of self-induced $A\beta_{42}$ aggregation

Inhibition of  $A\beta_{42}$  aggregation was measured using a Thioflavin T (ThT)-binding assay<sup>45</sup>. Resveratrol and curcumin were used as reference compounds. HFIP pretreated  $A\beta_{42}$  samples (Anaspec Inc) were resolubilized with a 50 mM phosphate buffer (pH 7.4) to give a 25  $\mu\text{M}$  solution. Each test compound was firstly prepared in DMSO at a concentration of 200  $\mu\text{M}$  and then 1  $\mu\text{L}$  of each was added to the well of black, opaque Corning 96-well plates such that the final solvent concentration was 10%. The final concentration of each compound was 20  $\mu\text{M}$ , which was prepared in

independent triplicates. The solvent control was also included. Then, 9  $\mu\text{L}$  of 25  $\mu\text{M}$   $A\beta_{42}$  sample was added to each well and the samples mixed by gentle trapping. Plates were covered to minimize evaporation and incubated in dark at room temperature for 46-48 h with no agitation. After the incubation period, 200  $\mu\text{L}$  of 5  $\mu\text{M}$  ThT in 50 mM glycine-NaOH buffer (pH 8.0) was added to each well. Fluorescence was measured on a SpectraMax M5 multi-mode plate reader (Molecular Devices, Sunnyvale, CA, USA) with excitation and emission wavelengths of 446 nm and 490 nm, respectively. The fluorescence intensities were compared and the percent inhibition due to the presence of the inhibitor was calculated by the following formula:  $100 - (IF_i/IF_o \times 100)$ , where  $IF_i$  and  $IF_o$  are the fluorescence intensities obtained for  $A\beta_{42}$  in the presence and in the absence of inhibitor, respectively, minus the fluorescence intensities due to the respective blanks.

#### 4.2.4. *In vitro* inhibition of Monoamine oxidase

Human MAO-A and MAO-B were purchased from Sigma-Aldrich. The capacity of the test compounds to inhibit hMAO-A and hMAO-B activities was assessed by Amplex Red MAO assay<sup>47</sup>. Briefly, 0.1 mL of sodium phosphate buffer (0.05 M, pH 7.4) containing the tested drugs at various concentrations and adequate amounts of recombinant hMAO-A or hMAO-B required and adjusted to obtain in our experimental conditions the same reaction velocity, i.e., to oxidize (in the control group) the same concentration of substrate: 165 pmol of *p*-tyramine/min (MAO-A: 1.1  $\mu\text{g}$  protein; specific activity: 150nmol of *p*-tyramine oxidized to *p*-hydroxyphenylacetaldehyde /min/mg protein; MAO-B: 7.5  $\mu\text{g}$  protein; specific

activity: 22 nmol of *p*-tyramine transformed/min/mg protein) were incubated for 15 min at 37 °C in a flat-black-bottom 96-well microtest plate placed in a dark fluorimeter chamber. After this incubation period, the reaction was started by adding 200 μM (final concentrations) Amplex Red reagent, 1 U/mL horseradish peroxidase, and 1 mM *p*-tyramine. The production of H<sub>2</sub>O<sub>2</sub> and consequently, of resorufin, was quantified at 37 °C in a SpectraMax Paradigm (Molecular Devices, Sunnyvale, CA) multi-mode detection platform reader based on the fluorescence generated (excitation, 545 nm; emission, 590 nm). The specific fluorescence emission was calculated after subtraction of the background activity. The background activity was determined from wells containing all components except the MAO isoforms, which were replaced by a sodium phosphate buffer solution (0.05 M, pH 7.4). The percent inhibition was calculated by the following expression:  $(1 - IF_i/IF_c) \times 100$  in which *IF<sub>i</sub>* and *IF<sub>c</sub>* are the fluorescence intensities obtained for MAO in the presence and absence of inhibitors after subtracting the respective background.

#### 4.2.5. Reversibility and Kinetic studies of hMAO-B inhibition

To determine whether the inhibition of MAO-B by the 6-substituted 3-arylcoumarin derivatives were reversible or irreversible, the time-dependence of inhibition of a selected inhibitor **5p** was examined. Compound **5p** was allowed to pre-incubate with recombinant human MAO-B for various periods of time (0, 15, 30, 60 min) at 37 °C in potassium phosphate buffer (0.05 M, pH 7.4). The concentration of **5p** was equal to two-fold the measured IC<sub>50</sub> value for the inhibition of hMAO-B. The reactions were subsequently diluted two-fold to yield a final enzyme concentration of 0.015 mg/mL

and concentrations of the **5p** that are equal to the  $IC_{50}$  values. The reactions were incubated at 37 °C for a further 15 min. All measurements were carried out in triplicate and are expressed as mean  $\pm$  SD.

To obtain of the mechanism of action **5p**, reciprocal plots of 1/velocity versus 1/substrate were constructed at different concentrations of the substrate *p*-tyramine (50-500  $\mu$ M) by using Ellman's method. Four different concentrations of **5p** (0, 0.1, 0.2 and 0.4  $\mu$ M) were selected for the kinetic analysis of hMAO-B inhibition. The plots were assessed by a weighted least-squares analysis that assumed the variance of velocity (*v*) to be a constant percentage of *v* for the entire data set. Slopes of these reciprocal plots were then plotted against the concentration of **5p** in a weighted analysis. Data analysis was performed with Graph Pad Prism 4.03 software (Graph Pad Software Inc.).

#### 4.2.6. *Molecular docking study*

To study the binding details of compound **5p** with hAChE and hMAO-B, docking study was performed using the Molecular Operating Environment (MOE 2008.10) software package, and the Marvin software package ([http:// www.chemaxon.com](http://www.chemaxon.com)) was carried out to calculate the protonation level of the ligand in physiological pH. The X-ray crystal structure of the hAChE (PDB 4EY7) and hMAO-B (PDB 2V61) were applied to build the starting model, which were obtained from the Protein Data Bank ([www.rcsb.org](http://www.rcsb.org)). Heteroatoms and water molecules in the PDB files were removed and all hydrogen atoms were subsequently added to the proteins. Compound **5p** was drawn in MOE. The compound was then protonated using the protonate 3D protocol

and energy was minimized using the MMFF94x force field in MOE. After the enzymes and compound **5p** were ready for the docking study, **5p** was docked into the active site of the protein by the “Triangle Matcher” method. The Dock scoring in MOE software was done using ASE scoring function and Forcefield was selected as the refinement method. The best 10 poses of molecules were retained and scored. After docking, the geometry of resulting complex was studied using the MOE’s pose viewer utility.

#### 4.2.7. *ABTS assay*

ABTS radical cation scavenging method was described as follow: 2, 2’-Azino-bis-2-ethybenz-thiazoline-6-sulfonic acid (ABTS) was dissolved in purified water to a 7 mM concentration. ABTS radical cation (ABTS<sup>•+</sup>) was produced by reacting ABTS stock solution with 2.45 mM potassium persulfate (final concentration) and allowing the mixture to stand in the dark at room temperature for at least 18 h before use. The stock solution of ABTS was serially diluted with sodium phosphate buffer (50 mM, pH 7.4) to 100  $\mu$ M. Trolox and all target compounds at different concentrations (total volume of 50  $\mu$ L) were added to 150  $\mu$ L of 100  $\mu$ M ABTS solution, respectively. After the addition of either trolox or another antioxidant to the ABTS solution, complete mixing of reactants was achieved by bubbling three to four times using plastic pipettes. The optical absorbance of ABTS at 415 nm was measured at 6 min after addition and equilibrated at 30 °C. Each individual treatment was repeated for three times and the results of the experiments were compared.

#### 4.2.8. *In vitro blood-brain barrier permeation assay*

Brain penetration of compounds was evaluated using a parallel artificial membrane permeation assay (PAMPA) in a similar manner as described by Di *et al*<sup>53</sup>. Commercial drugs were purchased from Sigma and Alfa Aesar. The porcine brain lipid (PBL) was obtained from Avanti Polar Lipids. The donor microplate (PVDF membrane, pore size 0.45  $\mu\text{m}$ ) and the acceptor microplate were both from Millipore. The 96-well UV plate (COSTAR@) was from Corning Incorporated. The acceptor 96-well microplate was filled with 300  $\mu\text{L}$  of PBS/EtOH (7:3), and the filter membrane was impregnated with 4  $\mu\text{L}$  of PBL in dodecane (20 mg/mL). Compounds were dissolved in DMSO at 5 mg/mL and diluted 50-fold in PBS/EtOH (7:3) to achieve a concentration of 100  $\mu\text{g}/\text{mL}$ , 200  $\mu\text{L}$  of which was added to the donor wells. The acceptor filter plate was carefully placed on the donor plate to form a sandwich, which was left undisturbed for 18 h at 25 °C. After incubation, the donor plate was carefully removed and the concentration of compound in the acceptor wells was determined using a UV plate reader (Flexstation@ 3). Every sample was analyzed at five wavelengths, in four wells, in at least three independent runs, and the results are given as the mean  $\pm$  standard deviation. In each experiment, 11 quality control standards of known BBB permeability were included to validate the analysis set.

#### 4.2.9. PC12 cells culture and cell viability assay

The toxicity effect of tested compounds on the rat pheochromocytoma (PC12) cells was examined according to the previous methods<sup>54, 55</sup>. The PC12 cells routinely grown at 37 °C in a humidified incubator with 5% CO<sub>2</sub> in Dulbecco's modified Eagle's medium (DMEM) supplemented with 10% bovine calf serum, 100 units/mL

penicillin, and 100 units/mL of streptomycin. The Cells were sub-cultured in 96-well plates at a seeding density of 10,000 cells per well and allowed to adhere and grow. When cells reached the required confluence, they were placed into serum-free medium and treated with compounds **5o** and **5p**. Twenty-four hours later the survival of cells was determined by MTT assay. Briefly, after incubation with 20  $\mu$ L of MTT at 37 °C for 4 h, living cells containing MTT formazan crystals were solubilized in 200  $\mu$ L DMSO. The absorbance of each well was measured using a microculture plate reader with a test wavelength of 570 nm and a reference wavelength of 630 nm. Results are expressed as the mean  $\pm$  SD of three independent experiments.

PC12 cells were seeded at  $5 \times 10^3$  cells/well in 96-well plates for neuroprotection activity assay. After 24 h, the medium was removed and replaced with the tested compounds (2.5, 5, 10, 20  $\mu$ M) at 37 °C and incubated for another 24 h. Melatonin was used as the control with the same concentrations of 2.5, 5, 10, 20  $\mu$ M. Then, the cells were exposed to  $A\beta_{42}$  (20  $\mu$ M) and incubated at 37 °C for 24 h before assayed with MTT. PC12 cells were cultured without tested compound or  $A\beta_{42}$  as control group and the results were expressed by percentage of control. Results are expressed as the mean  $\pm$  SD of three independent experiments.

### Abbreviations

AD, Alzheimer's disease; ChEs, cholinesterases; AChE, acetylcholinesterase; BuChE, butyrylcholinesterase; MAO, monoamine oxidase; CAS, catalytic active site; PAS, peripheral anionic site; APP, amyloid precursor protein; MTDL, multi-target-directed ligand; DCC, N, N'-dicyclohexylcarbodiimide; SI, selectivity index; Th-T,

Thioflavin-T; CNS, central nervous system; BBB, blood-brain barrier; PAMPA-BBB, parallel artificial membrane permeation assay for BBB; MTT, methyl thiazolyl tetrazolium.

### Acknowledgments

The research work was financially supported by the Project of National Natural Sciences Foundation of China (81573313), the Program for Changjiang Scholars and Innovative Research Team in University (PCSIRT-IRT\_15R63).

### References

- 1 M. Goedert and M. G. Spillantini, *Science*, 2006, **314**, 777-781.
- 2 A. Castro and A. Martinez, *Curr. Pharm Des.*, 2006, **12**, 4377-4387.
- 3 A. K. Ghosh, N. Kumaragurubaran and J. Tang, *Curr Top Med Chem.*, 2005, **5**, 1609-1622.
- 4 N. López, C. Tormo, I. De Blas, I. Llinares and J. Alom, *J. Alzheimer's Dis.*, 2013, **33**, 823-829.
- 5 V. Tumiatti, A. Minarini, M. Bolognesi, A. Milelli, M. Rosini and C. Melchiorre, *Curr Med Chem.*, 2010, **17**, 1825-1838.
- 6 P. Schelterns and H. Feldman, *Lancet Neurol.*, 2003, **2**, 539-547.
- 7 V. N. Talesa, *Mech Ageing Dev.*, 2001, **122**, 1961-1969.
- 8 P. B. Watkins, H. J. Zimmerman, M. J. Knapp, S. I. Gracon and K. W. Lewis, *Jama.*, 1994, **271**, 992-998.
- 9 R. J. Polinsky, *Clin Ther.*, 1998, **20**, 634-647.
- 10 L. J. Scott and K. L. Goa, *Drugs.*, 2000, **60**, 1095-1122.

- 11 W. Weyler, Y. -P. P. Hsu and X. O. Breakfield, *Pharmacol Ther.*, 1990, **47**, 391-417.
- 12 P. H. Axelsen, M. Harel, I. Silman and J. L. Sussman, *Protein Sci.*, 1994, **3**, 188-197.
- 13 L. Piazzzi, A. Rampa, A. Bisi, S. Gobbi, F. Belluti, A. Cavalli, M. Bartolini, V. Andrisano, P. Valenti and M. Recanatini, *J Med Chem.*, 2003, **46**, 2279-2282.
- 14 J. Hardy and D. J. Selkoe, *Science*, 2002, **297**, 353-356.
- 15 Y. Suzuki, J. R. Brender, M. T. Soper, J. Krishnamoorthy, Y. Zhou, B. T. Ruotolo, N. A. Kotov, A. Ramamoorthy and E. N. G. Marsh, *Biochemistry.*, 2013, **52**, 1903-1912.
- 16 R. Jakob - Roetne and H. Jacobsen, *Angew. Chem.-Int. Edit.*, 2009, **48**, 3030-3059.
- 17 M. Jucker and L. C. Walker, *Ann Neurol.*, 2011, **70**, 532-540.
- 18 N. S. Kumar and N. Nisha, *Chin J Nat Med.*, 2014, **12**, 801-818.
- 19 M. Youdim, J. Finberg and K. Tipton, Monamine oxidase, *Catecholamines I*, Springer., 1988, 119-192.
- 20 J. -Y. Mitoma and A. Ito, *J Biochem.*, 1992, **111**, 20-24.
- 21 S. -Y. Son, J. Ma, Y. Kondou, M. Yoshimura, E. Yamashita and T. Tsukihara, *Proc Natl Acad Sci.*, 2008, **105**, 5739-5744.
- 22 C. Binda, M. Li, F. Hubálek, N. Restelli, D. E. Edmondson and A. Mattevi, *Proc Natl Acad Sci.*, 2003, **100**, 9750-9755.
- 23 R. R. Ramsay, S. O. Sablin and T. P. Singer, *Prog Brain Res.*, 1995, **106**, 33-39.
- 24 M. Rosini, E. Simoni, M. Bartolini, A. Cavalli, L. Ceccarini, N. Pascu, D. W.

- McClymont, A. Tarozzi, M. L. Bolognesi and A. Minarini, *J Med Chem.*, 2008, **51**, 4381-4384.
- 25 R. León, A. G. Garcia and J. Marco-Contelles, *Med. Res. Rev.*, 2013, **33**, 139–189.
- 26 I. Bolea, J. Juárez-Jiménez, C. de los Ríos, M. Chioua, R.n. Pouplana, F. J. Luque, M. Unzeta, J. Marco-Contelles and A. Samadi, *J Med Chem.*, 2011, **54**, 8251-8270.
- 27 C. Lu, Y. Guo, J. Yan, Z. Luo, H. -B. Luo, M. Yan, L. Huang and X. Li, *J Med Chem.*, 2013, **56**, 5843-5859.
- 28 C. Lu, Q. Zhou, J. Yan, Z. Du, L. Huang and X. Li, *Eur J Med Chem.*, 2013, **62**, 745-753.
- 29 L. -F. Pan, X. -B. Wang, S. -S. Xie, S. -Y. Li and L. -Y. Kong, *MedChemComm.*, 2014, **5**, 609-616.
- 30 J. Sterling, Y. Herzig, T. Goren, N. Finkelstein, D. Lerner, W. Goldenberg, I. Miskolczi, S. Molnar, F. Rantal and T. Tamas, *J Med Chem.*, 2002, **45**, 5260-5279.
- 31 L. Wang, G. Esteban, M. Ojima, O. M. Bautista-Aguilera, T. Inokuchi, I. Moraleda, I. Iriepa, A. Samadi, M. B. Youdim and A. Romero, *Eur J Med Chem.*, 2014, **80**, 543-561.
- 32 A. Samadi, C. de los Ríos, I. Bolea, M. Chioua, I. Iriepa, I. Moraleda, M. Bartolini, V. Andrisano, E. Gálvez and C. Valderas, *Eur J Med Chem.*, 2012, **52**, 251-262.
- 33 L. Pisani, M. Catto, I. Giangreco, F. Leonetti, O. Nicolotti, A. Stefanachi, S. Cellamare and A. Carotti, *ChemMedChem.*, 2010, **5**, 1616-1630.

- 34 X. Zhou, X. -B. Wang, T. Wang, L. -Y. Kong, *Bioorg Med Chem.*, 2008, **16**, 8011-8021.
- 35 S. Rizzo, C. Riviere, L. Piazzzi, A. Bisi, S. Gobbi, M. Bartolini, V. Andrisano, F. Morroni, A. Tarozzi and J. -P. Monti, *J Med Chem.*, 2008, **51**, 2883-2886.
- 36 L. Novaroli, M. Reist, E. Favre, A. Carotti, M. Catto and P. -A. Carrupt, *Bioorg Med Chem.*, 2005, **13**, 6212-6217.
- 37 S. -S. Xie, X. -B. Wang, J. -Y. Li, L. Yang and L. -Y. Kong, *Eur. J Med Chem.*, 2013, **64**, 540-553.
- 38 D. D. Soto-Ortega, B. P. Murphy, F. J. Gonzalez-Velasquez, K. A. Wilson, F. Xie, Q. Wang and M. A. Moss, *Bioorg Med Chem.*, 2011, **19**, 2596-2602.
- 39 D. Viña, M. J. Matos, M. Yáñez, L. Santana and E. Uriarte, *MedChemComm.*, 2012, **3**, 213-218.
- 40 J. -S. Lan, L. -F. Pan, S. -S. Xie, X. -B. Wang and L. -Y. Kong, *MedChemComm.*, 2015, **6**, 1293-1302.
- 41 Z. -C. Xu, X. -B. Wang, W. -Y. Yu, S. -S. Xie, S. -Y. Li and L. -Y. Kong, *Bioorg Med Chem Lett.*, 2014, **24**, 2368-2373.
- 42 G. L. Ellman, K. D. Courtney, V. Andres and R. M. Featherstone, *Biochem Pharmacol.*, 1961, **7**, 88-95.
- 43 D. Alonso, I. Dorronsoro, L. Rubio, P. Munoz, E. García-Palomero, M. Del Monte, A. Bidon-Chanal, M. Orozco, F. Luque and A. Castro, *Bioorg Med Chem.*, 2005, **13**, 6588-6597.
- 44 A. Asadipour, M. Alipour, M. Jafari, M. Khoobi, S. Emami, H. Nadri, A.

- Sakhteman, A. Moradi, V. Sheibani and F. H. Moghadam, *Bioorg Med Chem.*, 2013, **70**, 623-630.
- 45 H. Naiki, K. Higuchi, K. Nakakuki and T. Takeda, *Lab Invest.*, 1991, **65**, 104-110.
- 46 G. Stege, K. Renkawek, P. Overkamp, P. Verschuure, A. Van Rijk, A. Reijnen-Aalbers, W. Boelens, G. Bosman and W. De Jong, *Biochem Biophys Res Commun.*, 1999, **262**, 152-156.
- 47 N. Desideri, A. Bolasco, R. Fioravanti, L. Proietti Monaco, F. Orallo, M. Yáñez, F. Ortuso and S. Alcaro, *J Med Chem.*, 2011, **54**, 2155-2164.
- 48 M. J. Matos, C. Terán, Y. Pérez-Castillo, E. Uriarte, L. Santana and D. Vina, *J Med Chem.*, 2011, **54**, 7127-7137.
- 49 J. Wang and D. E. Edmondson, *Biochemistry.*, 2011, **50**, 7710-7717.
- 50 T. Jones, D. Balsa, M. Unzeta and R. Ramsay, *J Neural Transm.*, 2007, **114**, 707-712.
- 51 N. J. Miller and C. A. Rice-Evans, *Free Radical Res.*, 1997, **26**, 195-199.
- 52 C. Chen and J. Yang, *Acta Pharmacol Sin.*, 2005, **26**, 500-512.
- 53 L. Di, E. H. Kerns, K. Fan, O. J. McConnell and G. T. Carter, *Eur J Med Chem.*, 2003, **38**, 223-232.
- 54 H. Zheng, M. B. Youdim and M. Fridkin, *J Med Chem.*, 2009, **52**, 4095-4098.
- 55 Q. Xie, H. Wang, Z. Xia, M. Lu, W. Zhang, X. Wang, W. Fu, Y. Tang, W. Sheng and W. Li, *J Med Chem.*, 2008, **51**, 2027-2036.

## Legends

**Table 1.** Inhibition of eeAChE, eqBuChE and self-induced  $A\beta_{42}$  aggregation activities of the synthesized compounds.

**Table 2.** Inhibition of human ChEs activities.

**Table 3.** Human MAO-A, MAO-B Inhibition and ABTS assay of the synthesized compounds.

**Table 4.** Permeability results ( $Pe \times 10^{-6} \text{ cm s}^{-1}$ ) from the PAMPA-BBB assay for selected compounds with their predicted penetration into the CNS.

**Scheme 1.** Synthesis of 6-substituted 3-arylcoumarin derivatives. Reagents and conditions: (i) DCC, DMSO, 110 °C, 24-48 h; (ii)  $\alpha, \omega$ -dibromoalkanes,  $K_2CO_3$ , acetonitrile, 50 °C, 6 h; (iii) amines,  $K_2CO_3$ , acetonitrile, reflux, 8 h.

**Figure 1.** Structures of some reported ChE/MAO dual inhibitors.

**Figure 2.** Design strategy of the ChE/MAO dual inhibitors.

**Figure 3.** Kinetic study on the mechanism of hAChE inhibition by compound **5p**. Overlaid Lineweaver–Burk reciprocal plots of hAChE initial velocity at increasing substrate concentration (0.05-0.50 mM) in the absence of inhibitor and in the presence of **5p** are shown. Lines were derived from a weighted least-squares analysis of the data points.

**Figure 4.** (A) 2D and (B) 3D docking models of compound **5p** with hAChE generated with MOE. Atom colors: yellow-carbon atoms of **5p**, gray-carbon atoms of residues of hAChE, dark blue-nitrogen atoms, red-oxygen atoms. The dashed lines represent the interactions between the protein and the ligand.

**Figure 5.** Reversibility studies of hMAO-B inhibition by compound **5p**. Time-dependence inhibition was studied at several times of pre-incubation (0-60 min) of hMAO-B with compound **5p**.

**Figure 6.** Kinetic study on the mechanism of hMAO-B inhibition by **5p**. Overlaid Lineweaver-Burk reciprocal plots of hMAO-B initial velocity at increasing substrate concentration (0.05-1 mM) in the absence of inhibitor and in the presence of **5p** are shown. Lines were derived from a weighted least-squares analysis of the data points.

**Figure 7.** (A) 2D and (B) 3D docking models of compound **5p** with hMAO-B generated with MOE. Atom colors: yellow-carbon atoms of **5p**, gray-carbon atoms of residues of hMAO-B, dark blue-nitrogen atoms, red-oxygen atoms. The dashed lines represent the interactions between the protein and the ligand.

**Figure 8.** The Cell viability of compounds **5o** and **5p** in PC12 cells at 3.125-50  $\mu$ M.

**Figure 9.** Neuroprotection against  $A\beta_{42}$  toxicity. Compounds **5o** and **5p** were tested for neuroprotective activity against  $A\beta_{42}$  toxicity in PC12 neuroblastoma cells. Melatonin (10  $\mu$ M) was used as the reference compound. Results are expressed as percent viability compared to cells not treated with  $A\beta_{42}$ . Data represent the mean  $\pm$  SD of three observations. \*\*\* $p < 0.001$ , \*\* $p < 0.01$ , \* $p < 0.05$ .

**Table 1.** Inhibition of eeAChE, eqBuChE and self-induced  $A\beta_{42}$  aggregation activities of the synthesized compounds ( $R^2$  were showed in Scheme 1).

Compd	$R^1$	$R^2$	n	$IC_{50}$ ( $\mu M$ ) <sup>a)</sup>		Selectivity Index <sup>b)</sup>	Self-induced $A\beta_{42}$ aggregation inhibition <sup>c)</sup> (%)
				eeAChE	eqBuChE		
<b>5a</b>	CH <sub>3</sub>	A	2	2.81 ± 0.11	1.93 ± 0.07	0.687	72.5 ± 4.5
<b>5b</b>	CH <sub>3</sub>	A	3	4.64 ± 0.17	2.27 ± 0.12	0.489	45.3 ± 2.7
<b>5c</b>	CH <sub>3</sub>	A	4	15.9 ± 0.4	2.26 ± 0.09	0.142	50.1 ± 2.6
<b>5d</b>	CH <sub>3</sub>	A	5	17.3 ± 0.9	2.91 ± 0.07	0.168	62.1 ± 4.0
<b>5e</b>	CH <sub>3</sub>	B	2	4.72 ± 0.16	3.10 ± 0.14	0.657	55.3 ± 6.6
<b>5f</b>	CH <sub>3</sub>	C	2	5.44 ± 0.29	2.74 ± 0.13	0.504	43.2 ± 5.5
<b>5g</b>	CH <sub>3</sub>	D	2	5.61 ± 0.12	8.21 ± 0.33	1.46	34.1 ± 3.4
<b>5h</b>	CH <sub>3</sub>	E	2	2.10 ± 0.06	2.12 ± 0.08	1.01	60.6 ± 7.1
<b>5i</b>	CH <sub>3</sub>	F	2	4.83 ± 0.21	13.4 ± 0.6	2.77	40.8 ± 1.1
<b>5j</b>	CH <sub>3</sub>	G	2	28.8 ± 1.0	17.6 ± 0.6	0.611	62.6 ± 4.8
<b>5k</b>	CH <sub>3</sub>	H	2	3.12 ± 0.13	1.63 ± 0.09	0.522	32.2 ± 1.6
<b>5l</b>	CH <sub>3</sub>	A	2	78.3 ± 2.3	4.37 ± 0.22	0.0558	21.2 ± 1.3
<b>5m</b>	CH <sub>3</sub>	E	2	51.9 ± 1.2	1.32 ± 0.10	0.0254	36.2 ± 2.1
<b>5n</b>	CH <sub>3</sub>	A	2	1.26 ± 0.07	8.74 ± 0.19	6.94	48.6 ± 1.7
<b>5o</b>	CH <sub>3</sub>	E	2	0.941 ± 0.080	3.96 ± 0.15	4.21	61.3 ± 4.1
<b>5p</b>	OCH <sub>3</sub>	A	2	0.962 ± 0.031	18.6 ± 0.8	19.3	52.1 ± 1.0
<b>5q</b>	OCH <sub>3</sub>	E	2	0.713 ± 0.031	9.12 ± 0.25	12.8	44.3 ± 2.1
<b>5r</b>	OCH <sub>3</sub>	H	2	3.67 ± 0.22	3.65 ± 0.29	0.994	60.7 ± 4.5
<b>5s</b>	Cl	A	2	0.884 ± 0.035	75.5 ± 3.4	85.8	84.9 ± 4.3
<b>5t</b>	Cl	E	2	4.13 ± 0.15	3.17 ± 0.12	0.767	68.1 ± 3.8
<b>3c</b>	CH <sub>3</sub>	p-OH		N <sup>d)</sup>	N	-	61.2 ± 1.4
<b>3d</b>	OCH <sub>3</sub>	p-OH		N	N	-	55.0 ± 2.1
<b>3e</b>	Cl	p-OH		N	N	-	60.6 ± 2.8
6-methylcoumarin				N	N	-	37.1 ± 1.3
<b>Tacrine</b>		-		0.207 ± 0.020	0.052 ± 0.001	0.251	n.t.
<b>Galantamine</b>		-		2.96 ± 0.13	14.6 ± 0.5	4.95	n.t.
<b>Resveratrol</b>		-		178 ± 35	789 ± 67	4.43	65.9 ± 2.2
<b>Curcumin</b>		-		n.t. <sup>e)</sup>	n.t.	-	53.2 ± 1.1

<sup>a)</sup>  $IC_{50}$ : 50% inhibitory concentration (means ± SEM of three experiments). <sup>b)</sup> Selectivity Index =  $IC_{50}$  (eqBuChE)/ $IC_{50}$  (eeAChE). <sup>c)</sup> Inhibition of self-induced and Ach-induced  $A\beta_{42}$  aggregation, the measurements were carried out in the presence of 20  $\mu M$  compounds (means ± SEM of three experiments). <sup>d)</sup> Inactive at 100  $\mu M$  (highest concentration tested), at higher concentrations the compounds precipitate. <sup>e)</sup> n.t.=not tested

**Table 2.** Inhibition of human ChEs activities <sup>a)</sup>.

Compounds	IC <sub>50</sub> (μM) <sup>b)</sup>		Selectivity Index <sup>c)</sup>
	hAChE	hBuChE	
<b>5a</b>	3.67 ± 0.13	3.83 ± 0.18	1.04
<b>5h</b>	1.26 ± 0.09	2.79 ± 0.11	2.21
<b>5n</b>	0.311 ± 0.010	41.3 ± 2.1	133
<b>5o</b>	0.195 ± 0.007	28.2 ± 1.3	145
<b>5p</b>	0.185 ± 0.003	33.7 ± 1.2	182
<b>5q</b>	0.0650 ± 0.0010	23.5 ± 0.6	363
<b>5s</b>	0.976 ± 0.018	56.3 ± 2.5	57.7
<b>5t</b>	2.81 ± 0.12	38.8 ± 1.1	13.8
Tacrine	0.467 ± 0.015	0.0391 ± 0.0021	0.0837

<sup>a)</sup> AChE from human erythrocytes and BuChE from human serum were used. <sup>b)</sup> IC<sub>50</sub>: 50% inhibitory concentration (means ± SEM of three experiments). <sup>c)</sup> Selectivity Index = IC<sub>50</sub> (hBuChE)/IC<sub>50</sub> (hAChE).

**Table 3.** Human MAO-A, MAO-B Inhibition and ABTS assay of the synthesized compounds.

Compounds	IC <sub>50</sub> (μM) <sup>a)</sup>		Selectivity Index <sup>b)</sup>	ABTS assay <sup>c)</sup>
	hMAO-A	hMAO-B		
<b>5a</b>	N <sup>d)</sup>	0.218 ± 0.011	>459	0.77
<b>5b</b>	34.9 ± 1.4	0.905 ± 0.017	38.6	0.32
<b>5c</b>	26.7 ± 0.9	1.13 ± 0.04	23.6	0.35
<b>5d</b>	53.7 ± 1.2	9.87 ± 0.34	5.44	0.27
<b>5e</b>	N	8.26 ± 0.28	>12.11	0.48
<b>5f</b>	N	10.4 ± 0.3	>9.57	0.63
<b>5g</b>	N	13.0 ± 0.5	>7.68	0.51
<b>5h</b>	25.4 ± 0.5	6.75 ± 0.15	3.76	0.37
<b>5i</b>	N	12.9 ± 0.4	>7.75	0.63
<b>5j</b>	9.72 ± 0.31	3.17 ± 0.09	3.07	0.49
<b>5k</b>	N	4.36 ± 0.12	>22.9	0.68
<b>5l</b>	N	31.1 ± 1.2	>3.22	0.73
<b>5m</b>	N	25.7 ± 0.8	>3.89	0.36
<b>5n</b>	22.4 ± 1.1	0.743 ± 0.047	30.1	0.74
<b>5o</b>	1.57 ± 0.08	0.0635 ± 0.0024	24.7	0.81
<b>5p</b>	N	0.196 ± 0.012	>510	1.17
<b>5q</b>	51.9 ± 2.6	0.758 ± 0.035	68.5	0.92
<b>5r</b>	N	10.9 ± 1.1	9.17	1.26
<b>5s</b>	1.31 ± 0.08	0.681 ± 0.082	1.92	0.72
<b>5t</b>	20.9 ± 1.7	1.53 ± 0.10	13.7	0.45
<b>3c</b>	N	0.364 ± 0.041	>274	n.t. <sup>e)</sup>
<b>3d</b>	N	0.942 ± 0.107	>106	n.t.
<b>3e</b>	N	1.26 ± 0.09	>79.4	n.t.
6-methylcoumarin	N	N	-	n.t.
Selegiline	76.5 ± 7.1	27.8 ± 4.2 nM	2752	n.t.
Clorgyline	8.15 ± 0.64 nM	82.0 ± 6.9	<0.0001	n.t.
Iproniazid	6.95 ± 0.85	8.12 ± 0.59	0.86	-

<sup>a)</sup> IC<sub>50</sub>: 50% inhibitory concentration (means ± SEM of three experiments). <sup>b)</sup> Selectivity Index = IC<sub>50</sub> (hMAO-A)/IC<sub>50</sub> (hMAO-B). <sup>c)</sup> Data are expressed as trolox equivalent, (mmol trolox)/(mmol tested compound). <sup>d)</sup> Inactive at 100 μM (highest concentration tested), at higher concentrations the compounds precipitate. <sup>e)</sup> n.t. means not tested.

**Table 4.** Permeability results ( $\text{Pe} \times 10^{-6} \text{ cm s}^{-1}$ ) from the PAMPA-BBB assay for selected compounds with their predicted penetration into the CNS.

Compounds	Permeability ( $\text{Pe} \times 10^{-6} \text{ cm s}^{-1}$ ) <sup>a)</sup>	Prediction
<b>5a</b>	$16.6 \pm 1.3$	CNS+
<b>5h</b>	$15.0 \pm 1.7$	CNS+
<b>5n</b>	$13.5 \pm 0.9$	CNS+
<b>5o</b>	$9.2 \pm 0.3$	CNS+
<b>5p</b>	$13.7 \pm 1.6$	CNS+
<b>5q</b>	$12.1 \pm 0.8$	CNS+

<sup>a)</sup> Data are the mean  $\pm$  SD of three independent experiments.



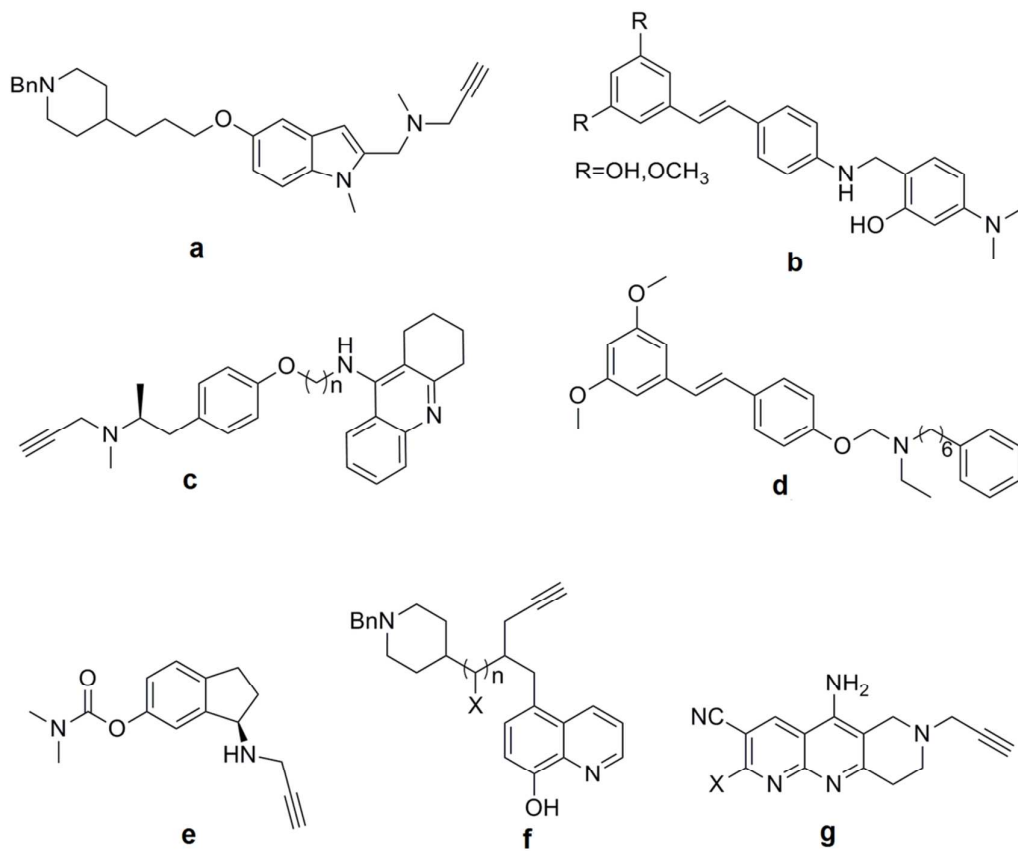


Figure 1.

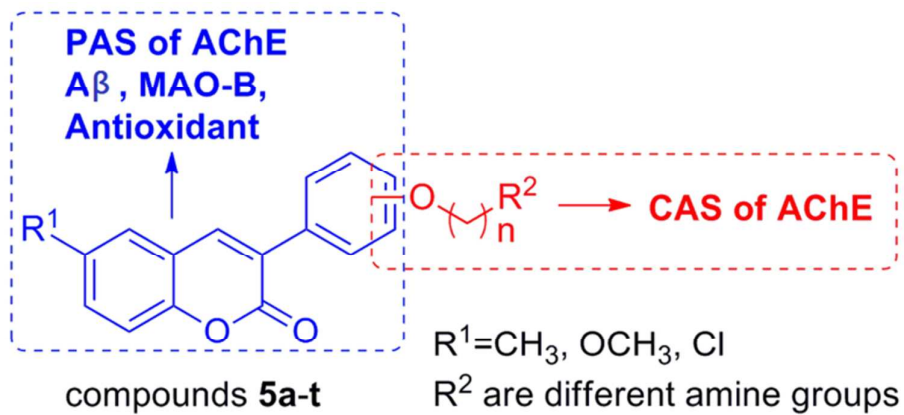


Figure 2.

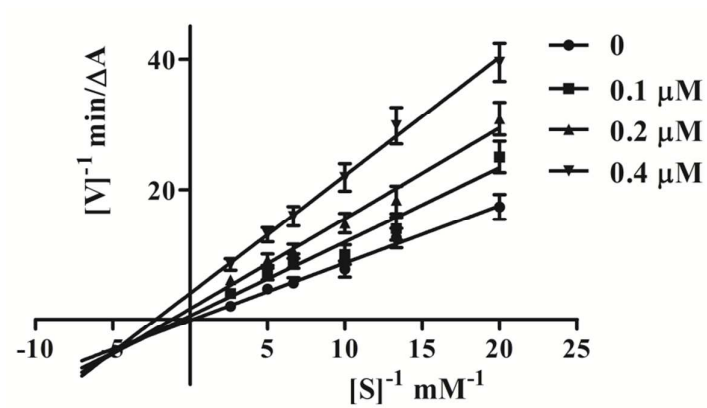


Figure 3.

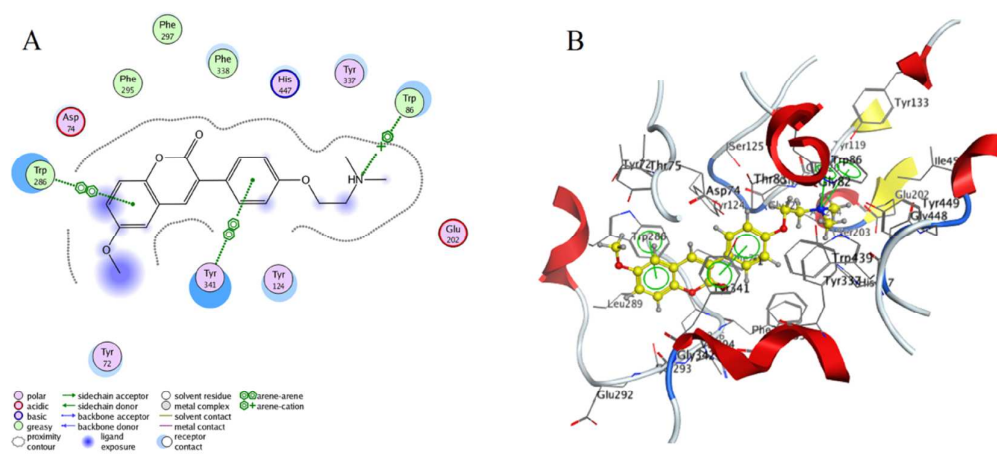


Figure 4.

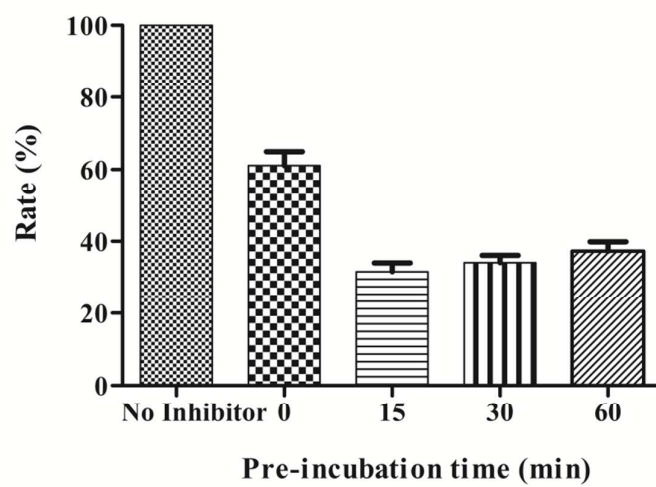


Figure 5.

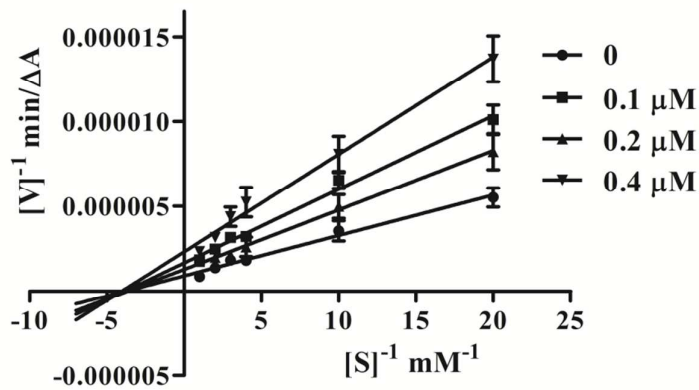


Figure 6.

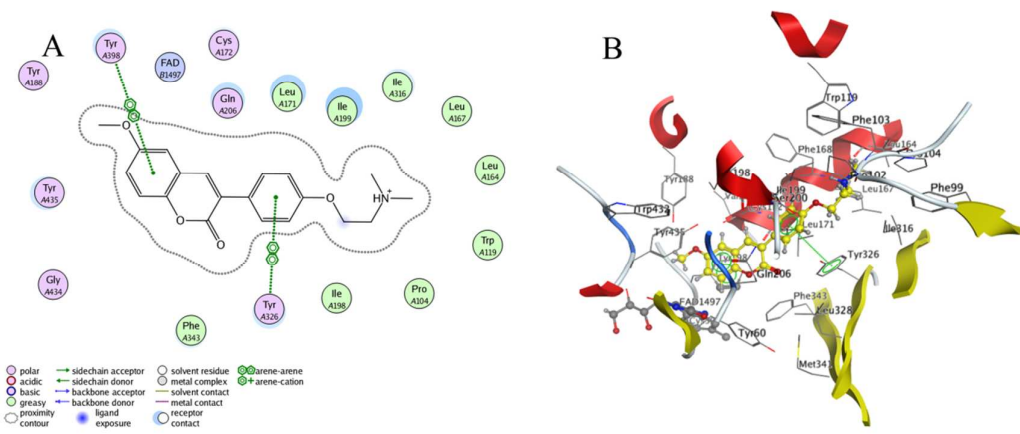


Figure 7.

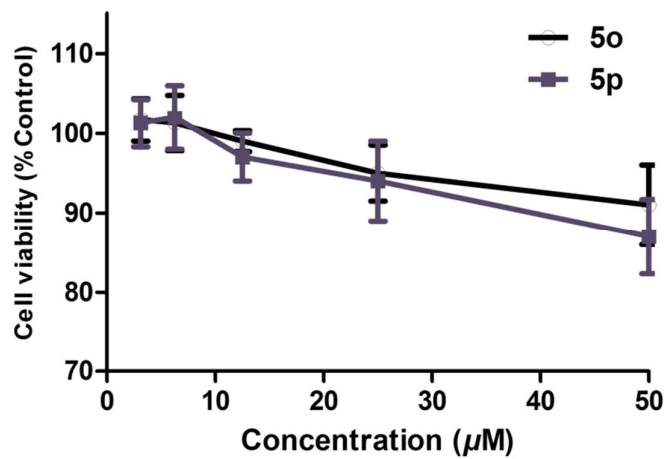


Figure 8.

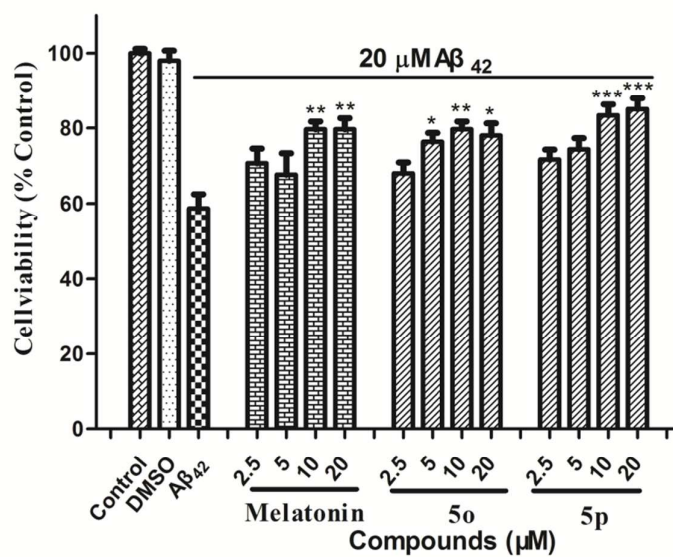


Figure 9.

Compounds **5o** and **5p** were both multifunctional hAChE/hMAO-B dual inhibitors for the treatment of AD.

